GROUND-MOTION PREDICTION EQUATIONS FOR SOUTHERN SPAIN AND SOUTHERN NORWAY OBTAINED USING THE COMPOSITE MODEL PERSPECTIVE

JOHN DOUGLAS[1]

Dept. Civil & Environmental Engineering, Imperial College London, SW7 2AZ, UK

HILMAR BUNGUM

NORSAR/ICG, POB 53, N-2027 Kjeller, Norway

FRANK SCHERBAUM

Inst. Geowissenschaften, Universität Potsdam, P.O. Box 601553, D-14415, Potsdam, Germany

Submitted 7th June 2005
Revised 4th October 2005

In this paper, two sets of earthquake ground motion relations to estimate peak ground and response spectral acceleration are developed for sites in southern Spain and in southern Norway using a recently published composite approach. For this purpose seven empirical ground motion relations developed from recorded strong-motion data from different parts of the world were employed. The different relations were first adjusted based on a number of transformations to convert the differing choices of independent parameters to a single one. After these transformations, which include the scatter introduced, were performed, the equations were modified to account for differences between the host and the target regions using the stochastic method to compute the host-to-target conversion factors. Finally functions were fitted to the derived ground motion estimates to obtain sets of seven individual equations for use in probabilistic seismic hazard assessment for southern Spain and southern Norway. The relations are compared with local ones published for the two regions. The composite methodology calls for the setup of independent logic trees for the median values and for the sigma values, in order to properly separate between epistemic and aleatory uncertainties after the corrections and the conversions.

Keywords: Ground motion estimation, stochastic method, attenuation relations, seismic hazard assessment, Spain, Norway.

[1] Now at: BRGM (ARN/RIS), 3 avenue C. Guillemin, BP 6009, F-45060 Orléans Cedex 2, France.

1 Introduction

Seismic hazard analyses are in general accompanied by considerable uncertainties that in part are aleatory (due to randomness) and in part epistemic (due to lack of knowledge). What drives the uncertainties the most varies considerably from case to case, dependent on how well the source, the path and the site effects are known, and it also strongly depends on the exceedance frequency (or return period). For most regions, however, the availability of local data and models for both source and site effects means that they are better known than path effects that are expressed through strong ground-motion models (so-called attenuation relations). The reason for this is simply that while seismicity data are available for most regions, strong-motion data are not. Given this, the way to solve this problem has traditionally been either to use relations from tectonically comparable regions, which are usually difficult to identify unambiguously, or to develop theoretical or calibrated-theoretical relations based, for example, on stochastic predictions. Criteria for such selection (and subsequent adjustments) of ground-motion relations has been discussed by Scherbaum et al. (2004a) and Cotton et al. (2005).

A different approach is to develop relations by modifying existing empirical strong-motion models on the basis of quantified seismotectonic differences between a host region (where the relation comes from) and a target region (where the relation is transported to), as demonstrated recently by Campbell (2003, 2004), who developed a hybrid technique and applied it between western and eastern North America. The use of a logic-tree approach (Bommer et al., 2005) is essential here since this facilitates solutions based on a number of relations, with proper treatment of uncertainties.

In the present study this problem is approached in a general and comprehensive way, following the methodology of Scherbaum et al. (2005a). This approach implies, for each magnitude, distance, and frequency of interest, to focus on the overall degree-of-belief in a particular ground-motion median level and a particular ground-motion variability as represented by the corresponding logic trees, one for the median and one for the aleatory variability. For this purpose a new data set is generated from each of these trees, corresponding to the scenarios defined by the different paths through it. In effect, new ground-motion models are generated in which all conversions and their assumed uncertainties are quantitatively incorporated and each empirical model contributes to the weight given to it by the analyst in each contributing magnitude, distance, and frequency bin. In the approach of

Scherbaum et al. (2005a) the ground motion sections of a complete logic tree for seismic hazard is therefore treated as a single composite model representing the complete state-of-knowledge-and-belief of a particular analyst on ground motion in a particular target region. Also, the quantiles of the composite ground motion models can provide the hazard analyst and the decision maker with a simple, clear and quantitative representation of the overall physical meaning of the ground-motion section of a logic tree and the accompanying epistemic uncertainty.

In the present application of this method, we firstly demonstrate the different steps required for the derivation of composite equations for a target region (Bommer et al., 2005; Scherbaum et al., 2005a), using southern Spain and southern Norway as examples. Then, using this methodology, two sets of equations are derived that can be used to predict ground motions in these two regions, within a seismic hazard analysis context. The sets of equations are based on fully compatible independent and dependent parameters, which subsequently can be used as branches within a logic tree in order to incorporate the effect of epistemic uncertainty. While the medians are covered in one logic tree, a different one is needed for the sigma values.

One purpose of this article is to demonstrate the difficulties encountered in estimating the parameters required to reliably characterise the target region. Therefore in sections 3.1 (southern Spain) and 3.2 (southern Norway) we careful review the existing literature that can be used to estimate the required target region parameters. These sections are required since they show that, even for reasonably well-studied areas such as Spain and Norway, it is necessary to consider the epistemic uncertainties in the characterisation of the target region, by including multiple options for the most important factors in the target region model. One problem that is not considered in this article is that due to possible correlations in the variables used in the models for the target regions, for example the correlation between the geometric spreading decay rate and the anelastic decay coefficients. For simplicity we assume that all our multiple target region models are independent, however, future applications of the methodology should perhaps consider the dependency between models.

2 Methodology and Approach

The method followed to derive ground motion estimation equations here (Scherbaum et al., 2005a) is inspired by the hybrid empirical technique of Campbell (2003, 2004). In this technique ground motion relations derived using strong-motion data from a host region are transformed via host-to-target conversion factors so as to model the expected ground motions in the target region [in Campbell (2003, 2004) these regions were western and eastern North America, respectively]. The host-to-target conversion factors are simply equal to the response spectral ratio between the ground motion estimated using the stochastic method (Boore, 1983; 2003) for the target region and the host region. The stochastic method can be applied to the target region because it does not rely on the availability of large quantities of strong-motion data of engineering significance, in contrast to what is needed for the derivation of purely empirical ground motion estimates. Parameters required for the stochastic method, such as path attenuation, can be obtained from data from ordinary seismological networks.

A strength of the composite technique for the construction of ground motion models in target regions is that the large body of data and results from studies for the estimation of ground motions based on observed strong-motion data are used. Douglas (2003a) provides a review of a large number of such studies which, through the present method, provide a basis for ground motion estimates in areas lacking the necessary data for a purely empirical approach, provided that essential host-to-target conversions are applied.

Another advantage of the technique is that the epistemic uncertainty within empirical ground motion equations, which were derived using a variety of data, functional forms and regression methods, is transferred to the equations for the target region. Using a suite of ground motion relations for the target region derived using stochastic methods can underestimate the epistemic uncertainty because of similarities in the methods used (Campbell, 2003).

Campbell (2003, 2004) uses four equations from western North America that were derived using similar sets of strong-motion data. Therefore the epistemic uncertainty modelled by differences in the ground motions predicted by such equations may underestimate the true uncertainty. In view of this, in this study a number of ground motion

estimation equations from different host regions (western North America, Europe and the Middle East and Japan) have been used in the derivation of the composite equations in order that the epistemic uncertainty is not underestimated. The choice of ground-motion models used in this study is slightly subjective and may not be optimal and therefore the results may not completely account for all epistemic uncertainty.

Since the estimation of epistemic uncertainty is an important facet of probabilistic seismic hazard analysis (e.g. Stepp et al., 2001), in the methodological approach followed here it is included through the use of a suite of ground motion relations from different host regions. It is important, however, that this epistemic uncertainty is not combined with the aleatory uncertainty when probabilistic hazard analysis is performed (Budnitz et al., 1997). Each ground motion relation should be a branch of the logic tree with its own weights and aleatory uncertainty. Therefore in this study a set of equations for the target regions are derived (one for each host equation) that are fully compatible in terms of independent parameters, however with an adjustment by the host-to-target factors. These equations are derived by regression of the estimated ground motions (including their aleatory uncertainty) from each transformed host equation separately. These equations can be used in a probabilistic seismic hazard analysis once they have been assigned appropriate weights.

The distance metric chosen for this study is the distance to the surface projection of rupture (d_{jb}) (usually referred to as the Joyner-Boore distance) and the magnitude scale adopted is moment magnitude (M_w).

2.1 Unification of ground-motion models

Firstly ground motions for rock sites are estimated via a number of commonly-used equations having converted the user-specified magnitude and distance into the magnitude scale and distance metric required by the equation. This conversion is performed using a Monte Carlo simulation that retains the scatter introduced by undertaking these conversions. These estimated ground motions are then scaled using the ratio of the estimated host-to-target conversion factors derived using the stochastic method as implemented in SMSIM (Boore, 2003) and also by factors to include the effect of style-of-faulting and the choice of the method to combine the two horizontal components. Lastly these ground motions from each of the ground motion models are weighted using weighting functions that can depend on period, magnitude and distance to yield a composite model. These weighting functions are

not discussed here; see Scherbaum et al. (2005a) for a discussion of weights within a composite model.

2.1.1 Magnitude conversions

The ground motion estimation equations chosen for this study have used either M_s or M_w [or, for the model of Sabetta & Pugliese (1996), a combination of M_L and M_s, which is assumed to be consistent with M_w] to characterise the earthquake size. Therefore, it is necessary to convert the target magnitude values to correctly use the host equation if the host and target magnitude scales are different. This conversion involves some uncertainty, which is modelled as a normally distributed error with mean 0 and the standard deviation,σ, of the conversion formula.

The M_w-M_s conversion formula of Ambraseys & Free (1997) (their equation 5.3, which is applicable for earthquakes with h<30km) is used for the conversion from M_s to M_w. The formula is:

$$M_s = -5.8661 + 2.6662\,\mathrm{M_w} - 0.1148 M_w^2 \; ; \sigma = 0.182 \qquad (1)$$

Similarly, the M_s-M_w conversion formula of Ambraseys & Free (1997) (their equation 6.2 with P=0 so it is applicable for earthquakes with h<30km) is used for the conversion from M_w to M_s. The formula is:

$$M_w = 4.749 - 0.337 M_s + 0.093 M_s^2 ; \sigma = 0.150 \qquad (2)$$

2.1.2 Distance conversions

Many different distance metrics have been used to characterize the source-to-site distance in equations for the estimation of ground motions (e.g. Abrahamson & Shedlock, 1997; Douglas, 2003a). The host equations chosen for this study have used four different metrics: distance to the surface projection of the rupture (also called Joyner-Boore distance), distance to the rupture, hypocentral distance and distance to the seismogenic rupture. To be able to correctly combine the computed ground motions from each host equation conversions between the target and host metrics need to be made (Scherbaum et al., 2004b). This conversion is not exact because of the finite extent of the earthquake source and since the location of the hypocentre on the rupture plane is unknown for future earthquakes. Therefore a Monte Carlo conversion procedure has been adopted using the technique given in

Scherbaum et al. (2004b) and using distance conversion coefficients developed specifically for the target regions based on the depth, mechanism and dip angle distributions in the target regions.

2.1.3 Style-of-faulting conversions

To derive ground motion estimates for the target region that may have a different predominant faulting mechanism than the host regions, it is important to apply a correction for the style-of-faulting for which the host equation applies. The ground motions predicted by those equations that are for a non-specified faulting mechanism are only strictly applicable for the target region if the distribution of earthquakes within the region with respect to faulting mechanism matches that in the host region of the equation. The method proposed by Bommer et al. (2003) has been adopted to make the conversion from generic to specific style-of-faulting. For those equations that have coefficients for the prediction of strike-slip or reverse ground motions, strike-slip motions are computed and then these motions are transformed to the requested faulting mechanism based on the same factors used to convert the equations for generic style-of-faulting. This has been done to retain a consistency between the motions predicted by equations for mechanism-dependent and mechanism-independent equations and also because it has been shown (Bommer et al., 2003) that the mechanism classification scheme adopted has a significant impact on the factors between ground motions from earthquakes with different mechanisms.

The factors used for conversion between ground motions predicted for earthquakes with different styles-of-faulting are taken from Bommer et al. (2003) who have taken their average factor $F_{R:SS}$ (where $F_{mech:SS}$ means the factor for converting from strike-slip motions to motions from an earthquake with 'mech' style-of-faulting) from Boore et al. (1997) and the upper and lower values of $F_{R:SS}$ are the average factors±10%. The factor $F_{N:SS}$ is 0.95 for all periods and the upper and lower factors are 1.00 and 0.90 respectively.

2.1.4 Component combination conversions

The chosen equations combine ground motions from the two horizontal components in four different ways: some use the larger horizontal component at all periods, one uses the spectral acceleration from the component that has the largest peak ground acceleration, some use the geometrical mean of the ground motions from the two components and some use both horizontal components as if they were independent. These different techniques for

combining the motions lead to differences in the computed ground motions and also differences in the associated standard deviations (e.g. Douglas, 2001; Bommer et al, 2005). Douglas (2001) computes a set of equations for the prediction of near-field peak ground accelerations and spectral ordinates using seven different methods for combining the two horizontal components. He finds that the standard deviations between the equations using different combination methods do vary but not by much. For example, the largest difference is between the standard deviation of the equation, in common logarithms, derived using both or a randomly chosen component, which is equal to about 0.30 at T=2s, and that of the equation derived using the geometric or arithmetic mean or the vectorial addition of the two components, which is equal to about 0.27 at T=2s. Therefore the increase in uncertainty is a factor of about 7%. The increase in uncertainty going from geometric to larger horizontal component is about 2%. Adjustments should therefore, in theory, be applied to the standard deviations to account for such differences but no such adjustments have been made here.

The factors to convert between ground motions estimated using different methods to combine the two horizontal components are presented in Bommer et al. (2005). Since there is some uncertainty in the estimation of the mean factor for converting between ground motions estimated using one technique and those estimated using another three branches have been used. The upper and lower estimates of the component conversion factors are the average factors±5%.

2.1.5 Host-to-target conversion using the stochastic method

The host-to-target conversion factors are derived using the stochastic method (e.g. Boore, 1983) as implemented in SMSIM (Boore, 2003). An estimate of the ground motion in the host region is computed using the stochastic method and the stochastic model for the host region, and a similar estimate is made for the target region using the stochastic model for the target region including the weighting for the different choices of parameters. The ratio of these two estimates is used to adjust the ground motion estimate for the host region derived using the empirical equations.

For the host region characterisation, stochastic models have been derived by inversion, using a genetic algorithm search, of synthetic data sets generated from the ground-motion models of interest (Scherbaum et al., 2005b). This method captures the model parameter variability as well as trade-offs by determining a whole set of “valid stochastic models” each of which fits the empirical ground-motion model to within the same misfit level. The models

of Scherbaum et al. (2005b) using hypocentral distance were used here since Scherbaum et al. (2005b) find that hypocentral distance generally leads to the best fit, amongst all the distance metrics they investigated, between stochastic and empirical models. Therefore for those host equations that do not use M_w and hypocentral distance a conversion needs to be performed. These conversions are performed in the same way as specified above. This conversion introduces additional uncertainty into the procedure.

For distances greater than 70km, the stochastic estimates were scaled by the factor required to make the stochastic estimate at 70km equal to the median empirical estimates at 70km for the same magnitude. This technique was introduced by Campbell (2003, 2004) in order to extend the ground motion estimates from the empirical equations that are invalid for distances beyond 60-100km to greater distances.

The local site amplification factors have been calculated using the quarter-wavelength method (e.g. Boore & Joyner, 1997) for the adopted local site profiles.

2.2 The computer program: CHEEP

To apply the method presented above, a computer program called CHEEP (Composite Hybrid Equation Estimation Program) was written in FORTRAN. This program undertakes all the conversions necessary to derive composite ground motion relations. At present eight commonly-used sets of equations for the prediction of ground motions from shallow crustal earthquakes are contained within the program although new equations can be easily added. The program can be obtained, upon request, from the authors of this paper.

As a test of the program it was used to reproduce the hybrid ground motion relation of Campbell (2003, 2004), who converts ground motion predictions from four equations derived mainly from data from western North America (Abrahamson & Silva, 1997; Campbell, 1997; Campbell & Bozorgnia, 2003a, b; Sadigh et al., 1997) to ground motion predictions for eastern North America. Figure 1 shows the comparison between the ground motion predictions obtained from the computer program written for this study and the predictions using the equations given in Campbell (2003, 2004). To make this comparison the same choices of host and target parameters were used. As can be seen from Figure 1, the program written for this study reproduces Campbell's predictions exactly within the error due to fitting of equations to the estimated ground motions.

2.3 Treatment of uncertainties

The basic idea behind the composite model perspective is to view the information represented by the ground-motion section of a logic tree within a ground-motion reference frame, not a model reference frame. In other words the purpose is to express degree-of-belief in ground-motion values, not in ground-motion models. The spread of the composite model as expressed by the distribution of its quantiles captures all the epistemic uncertainties represented by the logic-tree in a very transparent manner (Scherbaum et al., 2005a). Following the proposition of Budnitz et al. (1997), this is done separately for the median ground-motion values and the aleatory variabilities with the sources of uncertainties being treated in the composite model being different. For the median values the sources of uncertainties which are accommodated are: a) the spread of the original empirical models, b) the uncertainties from the different conversions, c) the bias of the best fitting stochastic model with respect to the empirical model, d) the uncertainties generated from the spread of all those stochastic models which are considered valid models, and e) the uncertainties coming from the stochastic characterisation of the target region. For the aleatory variabilities, only the uncertainties from the different conversions are accounted for; there currently being no model to incorporate the uncertainties due to the host-to-target conversions. A particular challenge in this context is the treatment of model parameter trade-offs and correlations. At present, these are only incorporated in the stochastic models for the host region (Scherbaum et al., 2005b) For the target regions, currently such models do not exist, this can be considered part of the overall epistemic uncertainty.

3 Case studies

In this section, two examples of the application of the method described above are presented. The two target regions chosen are southern Norway and southern Spain, both of which are areas of significant seismic hazard. However, both regions have little strong-motion data from which empirical ground-motion equations could be derived. Consequently they are good choices for the application of this procedure.

Andalusia, and in particular the area around the Granada basin in Spain, has significant earthquake activity. For example, Martín Martín (1989) finds expected MSK intensities at the 10^{-3} per year exceedance level to range from V-VI to IX in Granada itself. Udías & Muñoz (1979) find that the maximum intensity (MSK) of the 25th December 1884 earthquake south-

east of Granada was IX, corresponding to a magnitude of 6.7 to 7. It is therefore important for the expected ground motion in Andalusia to be carefully assessed.

Unfortunately little strong-motion data are available for this region, although there are a number of strong-motion instruments operating. There have been no ground-motion equations derived for this region except for those by Garcia-Fernandez & Canas (1991, 1995) based on data from short period analogue instruments. The data used for deriving these equations comes from earthquakes with magnitudes (m_{bLg}) less than or equal to 6, therefore extrapolating to larger magnitudes could create problems, also because of observed differences in the rate of decay of ground motions from small and large earthquakes (e.g. Douglas, 2003b).

Western Norway, the North Sea Rift and the mid-Norwegian passive continental margin are the most seismically active areas in northern Europe (Bungum et al., 1991, 2000; Byrkjeland et al., 2000). However, there are few strong-motion instruments operating and essentially no acceleration data available for earthquakes of any real engineering significance. Since most earthquakes occur offshore, most available accelerograms were recorded at large source-to-site distances, which means that it is difficult to constrain the near-field ground motions using normal regression techniques. The only published ground-motion equations that use data from Norway are those by Dahle et al. (1990, 1991) who derive equations for the estimation of pseudo-velocity. However, because the magnitude scaling in these equations is controlled by low-to-intermediate-magnitude seismological data at larger distances, these equations predict unreasonably large ground motions for short distances and large magnitudes.

In order to apply the stochastic method for the calculation of host-to-target conversion factors a number of parameters need to be defined for the target region. These parameters are (e.g. Boore, 2003): type of source spectrum, stress drop ($\Delta\sigma$), geometric attenuation, source duration, path duration, path attenuation, shear-wave velocity at the source, density at the source, local site diminution, and a local shear-wave velocity and density profile at the site. For the two regions considered here there is uncertainty associated with some of these parameters due to a lack of data and studies, essentially for the same reason that is behind the lack of strong-motion data in these regions.

The following two sections summarise the available information and present the parameters chosen for this study.

3.1 Southern Spain

The target area for southern Spain consists of rock sites within the Alpujárride complex bordering the eastern side of the Granada basin at about 37ºN-3.5ºW, in the Betic Cordillera. Computation of expected ground motions at this point will provide an expected bedrock motion that can be combined with the expected amplifications due to the sediments of the Granada basin.

The shear-wave velocity and density at the source should depend on the focal depth of the earthquakes. Most damaging earthquakes in this region are shallow crustal earthquakes with focal depths typically between 2 and 20km (see Figure 2). The CRUST2.0 model (Laske et al., 2003) provides estimates of crustal densities and velocities worldwide for a resolution of 2º × 2º. For depths between 12 and 22km in southern Spain this model gives a density of 2900 kg/m^3 and a velocity of 3.7km/s, which are similar to the commonly used values of 2800 kg/m^3 and 3.5km/s for western North America (e.g. Campbell, 2003). The CRUST2.0 values have been used here although slight variations in these parameters will not have a large impact on the computed ground motions.

Studies that have tried to fit spectral models to observed strong-motion spectra in this region (Morales et al., 1996; Morales et al., 2003) have used the Brune ω-square point source spectrum (e.g. Boore, 1983), which has been adopted also here. Other source spectra have been suggested, for example the double corner source spectrum of Atkinson & Boore (1998), which has been used in stochastic models for eastern North America. Due to a lack of evidence that these more complex source spectra are applicable in the two target regions studied here, it has been decided to use the simpler Brune ω-square point source spectrum. For a more complete discussion of this choice the reader is referred to Cotton et al. (2005). For the source duration the commonly assumed value of $1/f_0$, where f_0 is the corner frequency, has been adopted.

There are a few studies for this region that have addressed stress drops ($\Delta\sigma$), however most of these are based on microearthquakes (García-García et al., 1996; 2002). It is a matter of debate whether stress drops estimated from small magnitude earthquakes can be used for the simulation of ground motions from moderate and large earthquakes (Abercrombie, 1995; Mayeda & Walter, 1996; Ide & Beroza, 2001; Hiramatsu et al., 2002; Oye et al., 2005). García-García et al. (1996) find for magnitudes between 0.9 and 2.5 an

average moment-independent stress drop of about 0.02 MPa [0.2 bar]. If they allow M_0 to depend on $\Delta\sigma$ then they get a relation which would predict a $\Delta\sigma$ value of about 8800 MPa [88000 bar] at M_w=6, hence this equation clearly cannot be used outside its range of derivation. García-García et al. (2002) study 43 earthquakes with magnitudes between 1.4 and 3.5 and find that $\Delta\sigma$ varies between 0.005 and 0.36 MPa [0.05 and 3.6 bar]. Since both of these studies find much lower stress drops than are usually reported for moderate and large earthquakes the values from these studies will not be used here.

Mezcua et al. (1984) estimate the source radius of an earthquake of M_w=4.5 at Lorca on 6th June 1977 as 3.2km, leading to a $\Delta\sigma$ value of 0.07 MPa [0.7 bar]. Again this seems too low for larger magnitude earthquakes. However, Morales et al. (1996) find that 7.8 MPa [78 bar] gives a reasonable match to the observed spectra of two strong-motion records from 24th June 1984 earthquake and Morales et al. (2003) find $\Delta\sigma$=21.9 MPa [219 bar] and $\Delta\sigma$=24.6 MPa [246 bar] provide a reasonable fit to a few strong-motion spectra of the 23rd December 1993 and the 4th January 1994 earthquakes, respectively. Since there is little data on $\Delta\sigma$ from moderate and large earthquakes whose occurrence is important for seismic hazard assessment it has been decided to use three choices of $\Delta\sigma$ to account for this uncertainty and to cover the range of probable $\Delta\sigma$ values for this region. The three values used are 5, 10 and 20 MPa [50, 100 and 200 bar] with weights 0.3, 0.4 and 0.3, respectively.

For southern Spain there are also little data on the geometrical spreading of seismic waves, G(R). Morales et al. (1996) have used R^{-1} and Morales et al. (2003) have used R^{-1} for R<100km and $R^{-1/2}$ for greater distances when fitting the observed spectra with the Brune model. Ibáñez et al. (1993) find for direct S waves $G(R)=R^{-n}$, where $n=(1.19\pm0.04) \pm(0.057\pm0.007)f$ using data from between 15 and 78km. The Moho depth in this region is between 31 and 35km according to the CRUST2.0 (Laske et al., 2003) model. In comparison the Moho depth in eastern North America varies from 39 to 45km while in the most seismically active parts of California it varies from 27.5 to 34km (again from CRUST2.0). The depth to the Moho in southern Spain is therefore more similar to that in western North America, other differences (such as age and Q) notwithstanding, than to that in eastern North America. Therefore, since the geometrical spreading and path duration terms are related to the crustal structure it has been decided to use the geometrical spreading and path duration terms for western North America used by Campbell (2003, 2004), i.e. a decay of R^{-1} for distances up to 40km and $R^{-1/2}$ for greater distances, and a path duration of 0.05R.

The most well studied parameter that is required to construct a stochastic model for southern Spain is the quality factor Q, or the anelastic path attenuation. Mezcua et al. (1984) use aftershocks of the 6th June 1977 earthquake to estimate coda Q. For a frequency of 5Hz they get 320±43 for surface waves and 617±99 for body waves. Ibáñez et al. (1990) find a slight distance dependence of coda Q on focal depth; for a focal depth of 10-20km (the probable depth range of earthquakes in this region) they find $Q=112.5\pm8.4f^{0.85\pm0.03}$. Payo et al. (1990) find for the two (out of 17) regions closest to the target region Q=186 and Q=192 at 1Hz, while Pujades et al. (1990) find for the target region the relation $Q=100f^{0.6-0.8}$. In comparison Canas et al. (1991) find $Q_c=(98-208)f^{0.60-0.71}$ for frequencies between 1 and 5Hz, while De Miguel et al. (1992) give the equation $Q_{Lg}=(105\pm25)f^{0.93\pm0.14}$ for $1\leq f\leq18$Hz based on Lg waves. Akinci et al. (1995) compute estimates for attenuation due to scattering, intrinsic attenuation and total attenuation at given frequencies. Pujades et al. (1997) find the equation $Q_c=63f^{0.88}$ for an area to the east of the target region.

Figure 3 compares the estimated attenuation factors (i.e. $\exp(-\eta)$ where $\eta=\pi fR/\beta_c Q$ where f is frequency, R is hypocentral distance and β_c is shear-wave velocity) at 100km hypocentral distance from the published studies. It has been decided to use the five published studies that express Q(f) as a power law, each with weight 0.2 in order to capture the differences between the published attenuation models for southern Spain. The equations used are given in the figure caption.

Navarro et al. (1997) provide detailed shallow crustal structure shear-wave velocity profiles for the Almería region, which can be used to estimate the local shear wave velocity V_s at the site in question. The Alpujárride complex is in Navarro et al.'s region 4, for which a detailed profile down to 2km is given. The shear-wave velocity at the top of this profile is 1.87km/s. This profile, appended to the velocity and density model from CRUST2.0 (Laske et al., 2003) for this region, is used for the computation of the local site amplification factor. Zappone et al. (2000) provide details of laboratory measurements of P-wave velocities on rocks from the Betic chain. The measured P-wave velocities at the surface are between 5.60km/s and 7.00km/s; most of the velocities are between 5.8 and 6.1km/s (with densities between 2.7 and 2.75 gr/cm^3). These correspond to S-wave velocities between 3.3 and 3.5km/s. These are much higher than those estimated by Navarro et al. (1997), therefore the adoption of the Navarro et al. (1997) profile is a conservative assumption because it will estimate slightly higher amplification than would a profile with a V_s of 3.3-3.5km/s.

Estimates of κ for this region are again scarce. García-García et al. (1996) find κ in range 0.02 to 0.05s from acceleration spectra corrected for attenuation along path. García-García et al. (2002) examine 319 spectra from 43 earthquakes recorded at eight short-period seismic stations located on hard bedrock near the Granada basin and find that κ for P-waves is roughly from 0.01 to 0.04s and is from 0.006 to 0.04s for S-waves, with an average of 0.02s. Smaller values are from stations located on the hardest rock. They find no evidence for κ increasing with distance or any correlation with magnitude. Using the relation between κ and $V_{s,30}$ derived by Silva et al. (1998) ($\log \kappa = 1.6549 - 1.0930 \log V_{s,30}$ where $V_{s,30}$ is in m/s) gives a value of κ equal to 0.01s for $V_{s,30}$=1.9km/s (the adopted value for this study). Therefore for this study we have adopted three different choices of κ: 0.006, 0.02 and 0.05s (with weights 0.3, 0.4 and 0.3) to span the probable range.

Table 3 summarises the parameters used in the stochastic models for southern Spain.

3.1.1 Parameters required for generation of equations for distance conversion

To perform a correct conversion of distances between different metrics the focal depth, mechanism and dip angle distribution for earthquakes within the target region needs to be defined. For earthquakes in southern Spain, Stich et al. (2003) provide a catalogue of 48 moment tensor solutions that can be used to assess these distributions, occurring from 1984 to 2003 and within the area 36ºN-39ºN and 0-6ºW. Table 1 gives the distribution of the 45 shallow earthquakes from this catalogue with respect to faulting mechanism using the classification scheme of Frohlich & Apperson (1992). Almost two-thirds of the earthquakes are classified as odd, which corresponds to those earthquakes with oblique mechanisms or those whose mechanism cannot be decided unambiguously (Bommer et al., 2003). Most (62.5%) of the earthquakes that can be classified unambiguously are strike-slip. The ground motions from odd earthquakes cannot be modelled because none of the ground motion relations in the selected set has a category for such earthquakes. In view of these observations and because the null (B) axis of many of these odd earthquakes is plunging almost 60˚, thereby being close to strike-slip, it has been decided to assume for the purposes of this study that all earthquakes in the target region are strike-slip.

Figure 2 shows the depth distribution of the 45 shallow earthquakes from the catalogue of Stich et al. (2003), showing that most earthquakes occur in the upper 10km. Since the earthquakes located in the top 5km of the crust may be biased towards too shallow depths (reflecting a common problem with location algorithms), it has been decided to approximate

the depth distribution in southern Spain by two intervals, one for earthquakes with depths between 3 and 10km (73% of the earthquakes) and one for depths between 10 and 20km (27% of the earthquakes). There is no observable dependence of depth with magnitude, which is not surprising as the largest earthquake in the catalogue is M_w=5.1 and hence the observation that large earthquakes rupture at greater depth than small earthquakes is not likely to be seen. The dips of the simulated faults were chosen from a normal distribution with mean 75º and standard deviation 10º, truncated at 60º and 90º.

3.2 Norway

The target area in this case includes rock sites in southern Norway close to the most seismically active regions of Norway. The CRUST2.0 model (Laske et al., 2003) gives (for 62ºN, 4ºE near the most active offshore region) densities and shear-wave velocities of 3100kg/m^3 and 4km/s for depths between 21.5km and 32km, where the larger earthquakes in this region usually nucleate (Hansen et al., 1989). These values are used for the stochastic model for this region.

Kvamme et al. (1995) find that near-field earthquake spectra support the use of a source spectrum that falls off not steeper than ω-squared and possibly less steeply (a power of 1.5). Chael & Kromer (1988) study a mainshock-aftershock sequence that occurred off the western coast of Norway in 1986 (magnitudes 1.6 - 4.7), finding that the ω^2 model gives the best fit to the data. In a similar study based on two such sequences Bungum & Alsaker (1991) confirm the ω^2 model, but only if stress drop is assumed to be more or less independent of seismic moment. Moreover, two previous studies that have applied the stochastic method to this region (Singh et al., 1990; Bungum et al., 1992) have both adopted the ω^2 model for the source spectrum, hence it has also been used here. Both Singh et al. (1990) and Bungum et al. (1992) have used a source duration of $1/f_0$ where f_0 is the corner frequency, therefore this parameter has also been adopted here.

A number of previous studies have aimed at estimating stress drops ($\Delta\sigma$) for Norwegian earthquakes but as for southern Spain most of the earthquakes studied are small. Bungum et al. (1982) examine aftershocks of the 1978-1979 Meløy earthquake sequence with magnitudes (M_L) between -0.4 and 2.2 and find $\Delta\sigma$ between 0.06 to 2.21 MPa [0.6 to 22.1 bar]. They find that there is a strong dependency of $\Delta\sigma$ on M_0. Hansen et al. (1989) estimate stress drops for three larger earthquakes offshore of Norway, finding 5.5 MPa [55 bar] for an earthquake of M_w=4.7, 12.4 MPa [124 bar] for one of M_w=5.3 and 12.3 MPa [123 bar] for

one of M_w=5.2. Singh et al. (1990) find $\Delta\sigma$=10 MPa [100 bar] gives a match to the observed spectra of three large offshore earthquakes. Bungum & Alsaker (1991) compute $\Delta\sigma$ for two mainshocks - aftershocks sequences and find $\Delta\sigma$ equals 10.4 MPa [104 bar] for an M_L=4.8 mainshock, and 23.4 MPa [234 bar] for an M_L=4.9 mainshock, decreasing to 2.4 and 6.3 MPa [24 and 63 bar] for the weakest of the aftershocks. Kvamme et al. (1995) find, based on a large data base (M_L 1–5), that $\Delta\sigma$ are always below 10 MPa [100 bar] and most are below 1 MPa [10 bar] (the average is about 0.5 MPa [5 bar]) with evidence that $\Delta\sigma$ increases weakly with magnitude. Zobin & Havskov (1995) study 40 small (M_L=2.5-3.5) shallow earthquakes in area 59-63ºN, 2-8ºE, which contains both an extensional rift zone and a compressional margin zone. They find that for the margin zone: log $\Delta\sigma$=-1.44(±0.139)+0.116(±0.011) log M_0 and for the rift zone: log $\Delta\sigma$=-1.361(±0.44)+0.106(±0.033) log M_0, where M_0 is in Nm and $\Delta\sigma$ is in MPa. The margin zone earthquakes have greater stress drop than the rift zone events of the same moment and the difference increases with moment. An extrapolation to M_w=6 shows also here, however, that these equations cannot be used outside the magnitude range for which they were derived. Pačėsa (1999) finds that stress drops increase up to about M_w=3 and then are constant up to M_w=3.8, with values between 0.2 and 6.7 MPa [2 and 67 bar]. Chael & Kromer (1988) find that a constant stress drop model gives the best fit to the data, while Bungum & Alsaker find , partly based on the same data, that an ω^3 model combined with an increasing stress drop model fits the data almost equally well. Ottemöller & Havskov (2003) find $\Delta\sigma$ values between 0.04 and 6.05 MPa [0.4 and 60.5 bar] for Norwegian earthquakes between M_w=2.0 and 4.1, although they note (Ottemöller, written communication, 2003) that their estimates of $\Delta\sigma$ are uncertain due to the trade-off between corner frequency and near-surface attenuation particularly for small earthquakes.

The conclusion from this extensive review is that also for southern Norway there is little evidence available on which to base estimates of $\Delta\sigma$ for earthquakes of the size likely to cause ground motions of engineering significance. Therefore, as for southern Spain, three widely-separated values of $\Delta\sigma$ have been chosen: 5, 10 and 20 MPa [50, 100 and 200 bar] with weights 0.3, 0.4 and 0.3.

There are few studies and results available on the geometric spreading in Norway. Dahle et al. (1991) use r^{-1} for r<100km and $r^{-5/6}$ for greater distances. Kvamme et al. (1995) find that a decay of the form r^{-1} for distances r<200km and $r^{-1/2}$ for greater distances is appropriate

using simulations and a crustal structure for Scandinavia. The two previous studies using the stochastic method for this region (Singh et al., 1990; Bungum et al., 1992) have both adopted a decay of r^{-1} for distances r<100km and $r^{-1/2}$ for greater distances, as do Sereno et al. (1988). The depth to Moho in this region is between 32 and 40 km according to the CRUST2.0 (Laske et al., 2003) model, hence the depth to Moho in Norway is more similar to that in eastern North America than that in western North America. Therefore since the geometrical spreading and path duration terms are related to the crustal structure it has been decided to use the geometrical spreading and path duration terms for eastern North America derived by Atkinson & Boore (1998) and used by Campbell (2003, 2004), i.e. a decay of R^{-1} for distances up to 70 km, no decay from 70 to 130 km and $R^{-1/2}$ for distances greater than 130 km and a path duration of 0 up to 10km, 0.16R for distances between 10 and 70 km, -0.03R between 70 and 130 km and 0.04R for greater distances.

As for southern Spain, a number of studies have derived path attenuation functions for this region. Sereno et al. (1988) find $Q(f)=560f^{0.26}$ after assuming that the geometrical spreading of Lg waves is r^{-1} for r<100km and $r^{-1/2}$ for greater distances. Kvamme & Havskov (1989) give $Q(f)=127f^{1.08}$ for S-waves. Dahle et al. (1990) give $Q(f)=539+152f+1.43f^2$. Hansen et al. (1989) give $Q(f)=90+110f^{1.20}$. Singh et al. (1990) have used $Q(f)=290f$ from fitting the observed spectra of three larger offshore earthquakes, while Kvamme et al. (1995) give $Q(f)=438f^{0.71}$ for a Brune ω-square model with transition from r^{-1} to $r^{-1/2}$ at 200 km. Bungum et al. (1992) have used $Q(f)=465f^{0.64}$, which is from Kvamme et al. (1995) but for a transition distance of 100 km.

Figure 4 compares the estimated attenuation factors from the published studies for a hypocentral distance of 100 km, and shows that there are large differences between the behaviour of the different curves. For this study it has been decided to use the equation of Sereno et al. (1988), i.e. $Q(f)=560f^{0.26}$, with weight 0.5 and the equation of Kvamme et al. (1995), i.e. $Q(f)=438f^{0.71}$, with weight 0.5, since they roughly span range of published estimates.

The rock in the target region is granite or metamorphic rock, which has V_p values of between 4.5 and 5.5km/s (Grant & West, 1965, fig. 1-1, p. 8), which corresponds to V_s between 2.6 and 3.2km/s (by dividing by $\sqrt{3}$, corresponding to a Poisson's ratio of 0.25). Sjøgren et al. (1979) report the P-wave velocities in a gneiss-amphibolite-granite region (Vardeåsen), with a reasonably narrow distribution between 4.9 km/s and 6.1 km/s but with

about 10% of measured velocities below 4.9 km/s, corresponding to solid Precambrian rock masses broken by Permian tectonics. They also show similar velocities from other sites, and a mean calculated Poisson's ratio of 0.28, with little scatter. Therefore the range of V_s values is 2.7km/s to 3.4km/s. They also report V_p values for other sites with different rock types, with values of 6.0, 5.4, 4.8, 3.8, 4.1, 4.2, 4.4 and 4.7 km/s. Lokshtanov et al. (1991) estimate the velocity of the top layer at the NORSAR array. Their derived model for the shear-wave velocity has a layer of 1.02 km thick of average velocity 2.82 km/s overlying a half space of shear-wave velocity of 3.55 km/s. Since these surface shear-wave velocities are similar to that estimated by Boore & Joyner (1997) for eastern North America (i.e. $V_{s,30}$=2.8 km/s) Boore & Joyner's generic rock profile for eastern North America has been used to compute the site amplification for Norway.

There are very few estimates of κ for this region. Singh et al. (1990) find κ=0.025 gives a reasonable match to observed spectra of three large offshore earthquakes. Bungum et al. (1992) use an f_{max} of 40 Hz, which they adopt from eastern North America because of the lack of information. Kvamme et al. (1995) do not find evidence for an f_{max} (which has a similar role to κ) up to 50Hz. Pačėsa (1999) computes κ for nine stations (all located on hard rock) and find κ (they call it t*) equals 0.025 or 0.026 at all stations apart from BLS at which it is 0.030, which he suggests may be due to the presence of a large reservoir nearby. The average κ is 0.026, which comes from 388 data points. Using the relation between κ and $V_{s,30}$ derived by Silva et al. (1998) gives κ=0.008 for $V_{s,30}$=2.8 km/s (the value adopted for this region). Therefore for this study we have adopted three different choices of κ: 0.008, 0.017 and 0.026 with weights 0.3, 0.4 and 0.3 to span the probable range.

Table 3 summarises the parameters used in the stochastic models for southern Norway.

3.2.1 Parameters required for generation of equations for distance conversion

The catalogue of Hicks et al. (2000), which contains a compilation of 112 earthquake focal mechanism solutions for Norway and the North Sea, was used to assess the distribution of depths and focal mechanisms in the target area. All earthquakes in the region defined by 58-64ºN, 0-12ºE were considered. The 67 earthquakes in this region were classified using the scheme of Frohlich & Apperson (1992) (see Table 2). As for southern Spain a large proportion (47.8%) are classified as odd; these earthquakes have not been considered further. It is interesting that the proportion of earthquakes classified as odd in both southern Spain and Norway is much higher than that classified as odd by Bommer et al. (2003) using the

worldwide Harvard CMT catalogue for shallow earthquakes (64.4% and 47.8% compared with 16.2%). This could be because the focal mechanism catalogues of southern Spain and Norway solely contain mechanisms for small and moderate earthquakes (M_w<6), whose focal planes are more influenced by local stresses, structures and weakness zones, whereas the Harvard CMT catalogue consists mainly of mechanisms of moderate and large earthquakes ($M_W \geq 5.5$), whose focal planes usually reflect better the predominant stresses in the region. Table 2 shows that reverse earthquakes compose almost half (17 out of 35 earthquakes that are were not classified as odd, 48.5%) of the remaining earthquakes and strike-slip and normal compose 25.7% each. Therefore all three mechanisms are assumed to occur in this target region in the proportions 1:1:2 for normal: strike-slip: reverse. The dips of the normal simulated faults were chosen from a normal distribution with mean 60º and standard deviation 10º which is truncated at 45º and 75º. The dips of the simulated strike-slip faults were chosen from a normal distribution with mean 80º and standard deviation 10º which is truncated at 70º and 90º. The dips of the simulated thrust faults were chosen from a normal distribution with mean 45º and standard deviation 10º which is truncated at 30º and 60º.

The catalogue of Hicks et al. (2000) has also been used to assess the depth distribution of earthquakes with respect to style-of-faulting. Figure 5 shows that normal and strike-slip earthquakes occur reasonable uniformly at depths between 10 and 22km, therefore a uniform depth distribution has been used between those depths. It also shows that thrust earthquakes occur at all depths but more often at greater (≥18km) depths, therefore two uniform distributions have been used, one for depths between 4 and 18km (23.5% of thrust earthquakes) and one for between 18 and 34km (76.5% of thrust earthquakes).

3.3 Equations used for derivation of composite equations

For derivation of the composite equations for the two regions it was decided to use a number of published equations from different regions in order to capture the epistemic uncertainty in ground motion prediction. Only equations derived using observed strong-motion data were considered since the conversion of equations based on the stochastic method, such as Atkinson & Boore (1997), is not useful as the stochastic method could simply be directly applied to the target region rather than to derive host-to-target conversion factors.

Table 4 lists the equations chosen for this study and the choices made for the independent parameters in each equation. Each of the equations listed has its own set of

best-fit stochastic models, which are the models derived by Scherbaum et al. (2005b) using a new and objective genetic algorithm method to find the best-fitting models. This is in contrast to Campbell (2003) who assumed a single host stochastic model. For the purposes of this study it is assumed that pseudo-spectral acceleration, which is used to derive many of the chosen equations, and spectral acceleration, which is used to derive the rest of the chosen equations, are equal. This is a reasonable assumption except for long (>10s) periods (e.g. Chopra, 1995).

Ground motion estimates are computed at 14 periods, namely PGA, 0.02, 0.03, 0.05, 0.075, 0.10, 0.15, 0.20, 0.30, 0.50, 0.75, 1.0, 1.5 and 2.0s. Ground motion estimates were not computed for periods greater than 2.0s because coefficients for such predictions do not exist for the equations of Ambraseys et al. (1996) and Boore et al. (1997). For studies without an explicit equation for PGA (Abrahamson & Silva, 1997; Berge-Thierry et al., 2003; Lussou et al., 2001), spectral acceleration at the shortest period available (either 0.01, 0.02 or 0.03s) was assumed to be equal to PGA, even though this is not strictly valid. To compute ground motions at periods for which coefficients do not exist, linear interpolation of the coefficients was performed using the logarithms of the periods (Bommer et al., 2005). To estimate ground motions at periods shorter than the shortest period for which coefficients are available interpolations between the PGA (which is assumed to correspond to spectral acceleration at 0.01s) coefficients and the next shortest period spectral acceleration coefficients were performed. It should be noted that this method of interpolation could create some bias in the ground-motion estimates at short periods.

Ground motion estimates are computed for magnitudes from 4.5 to 7.5 in steps of 0.25 and for distances between 1 and 1000km at the same distances as Campbell (2003, 2004), namely 1, 2, 3, 5, 7, 10, 20, 30, 40, 50, 70, 100, 130, 200, 300, 500, 700 and 1000km (for distance greater than 70km the scaled stochastic estimates were used as mentioned above) for Norway and between 1 and 300km for southern Spain at the same distances. The estimates were computed up to 1000km for Norway, although it is unlikely that ground motions of engineering significance could be recorded at such distances, so as to make the regression analysis for the third branch of the trilinear decay function stable. For southern Spain, since a bilinear decay function has been adopted, ground motions only needed to be computed to 300km to make the regression analysis stable.

Estimated ground motions in the target region were fitted with curves using nonlinear least-squares regression to develop equations that are easier to use in seismic hazard analysis

than are individual point estimates for particular magnitudes and distances. Before the regression was performed the median estimated ground motion for each period, magnitude and distance was computed from the 100 samples so as not to introduce the epistemic variability due to the uncertainty in the host and target characterisation into the aleatory uncertainty of the derived target models.

3.4 Results for southern Spain

Since the geometric spreading function for the stochastic model for southern Spain includes a change of decay at 40km the functional form adopted to fit the individual estimates was modified from Campbell (2003, 2004)'s trilinear form to a bilinear form. The adopted functional form is:

$$\ln Y = c_1 + f_1(M_w) + f_2(M_w, d_{jb}) + f_3(d_{jb}) \qquad (3)$$

where:

$$f_1(M_w) = c_2 M_w + c_3(8.5 - M_w)^2$$
$$f_2(M_w, d_{jb}) = c_4 \ln R + (c_5 + c_6 M_w) d_{jb}$$
$$R = \sqrt{d_{jb}^2 + [c_7 \exp(c_8 M_w)]^2}$$

and:

$$f_3(d_{jb}) = 0 \text{ for } d_{jb} \leq r_1$$

$$f_3(d_{jb}) = c_9(\ln d_{jb} - \ln r_1) \text{ for } d_{jb} > r_1$$

where r_1=40km.

Equations were derived for each of the host equations, and the corresponding coefficients can be obtained from the authors on request. An example of the good fit between the ground motion estimates and the fitted equations is shown in Figure 6 for the converted Abrahamson & Silva (1997) equation.

Figure 7 gives an example of the effect of the host-to-target conversion factors for a magnitude M_w=6 earthquake at d_{jb}=20km in southern Spain. The graph shows the estimated response spectra from two sets of host equations (Abrahamson & Silva, 1997; Lussou et al., 2001) having unified the independent and dependent parameters (Sections 2.1.1 to 2.1.4) and estimated spectra for the target region (southern Spain) having applied the host-to-target conversion factors (Section 2.1.5). It shows that the effect of the host-to-target conversions is to bring the two estimated response spectra for the target region closer together than the

unconverted spectra, which are for two different host regions (western North America and Japan). The host-to-target conversions decrease the estimated spectral accelerations from the equations of Abrahamson & Silva (1997) at most periods whereas the conversion factors increase the estimated spectral accelerations from the equations of Lussou et al. (2001) at all periods. The largest conversion factor is about two.

Figure 8 shows the predicted PGAs and SA at 1s from a magnitude M_w=6 earthquake in southern Spain using the derived equations. Ground motions have been graphed for M_w=6 since it is within the magnitude range where all the host equations are applicable. These graphs show that the predicted median ground motions from each of the derived equations are similar.

Figure 9 shows the response spectra predicted using the derived equations for Spain for M_w=6 and d_{jb}=20km. This combination of magnitude and distance has been chosen to fall within the range of applicability of all the host equations. This graph shows that there is still significant variability in the predicted ground motions from each of the different equations. For example at 0.05s the predicted SAs vary between about 0.8ms^{-2} and 1.5ms^{-2} (a factor of roughly two times).

Figure 10 compares the predicted PGA from the derived composite equation for Spain to those predicted using the equations of Garcia-Fernandez & Canas (1991,1995) and Cabañas et al. (2000) for M_w=5 and 7. The graph shows that the predicted PGAs for M_w=5 are reasonably consistent between the three equations but for M_w=7 the two previously published equations predicted ground motions that are much too high. This is because no data from large magnitude earthquakes was used for their derivation.

3.5 Results for southern Norway

Since the geometric spreading and path duration functions used by Campbell (2003, 2004) for eastern North America were used here for Norway the functional form adopted by Campbell (2003, 2004) was used to fit the individual estimates. Therefore the equations have the form:

$$\ln Y = c_1 + f_1(M_w) + f_2(M_w, d_{jb}) + f_3(d_{jb}) \qquad (4)$$

where:

$$f_1(M_w) = c_2 M_w + c_3 (8.5 - M_w)^2$$
$$f_2(M_w, d_{jb}) = c_4 \ln R + (c_5 + c_6 M_w) d_{jb}$$
$$R = \sqrt{d_{jb}^2 + [c_7 \exp(c_8 M_w)]^2}$$

and:

$$f_3(d_{jb}) = 0 \text{ for } d_{jb} \leq r_1$$
$$f_3(d_{jb}) = c_9 (\ln d_{jb} - \ln r_1) \text{ for } r_1 < d_{jb} \leq r_2$$
$$f_3(d_{jb}) = c_9 (\ln d_{jb} - \ln r_1) + c_{10} (\ln d_{jb} - \ln r_2) \text{ for } d_{jb} > r_2$$

where r_1=70km and r_2=130km.

Figure 11 shows the predicted PGAs and SA at 1s from a magnitude M_w=6 earthquake in Norway using the derived equations for normal faulting earthquakes. These graphs show that the predicted ground motions from the derived equations are reasonably similar with more variability at short distances (d_{jb}<10km). There is also more variability in each of the models compared with those for Spain.

Figure 12 shows the response spectra predicted using the derived equations for Norway for M_w=6 and d_{jb}=20km. This graph is similar to that for Spain in terms of estimated SAs and also variability among the different models.

A comparison of the predicted ground motions given by two of the relations adopted for Norway for the three mechanisms and those predicted by the relations presented by Bungum et al. (1992) and Dahle et al. (1992) is shown in Figure 13. This figure shows that for M_w=5 the two equations predict reasonably similar ground motions to the previous published equations; however, for large magnitudes the previous published equations are not constrained and therefore the ground motions predicted by these relations are too high.

Figure 14 shows the effect of style-of-faulting on the predicted ground motions. For short distances the effect of shallower focal depths for normal and strike-slip faulting earthquakes compared with reverse faulting earthquakes means that the predicted ground motions in the near field are larger for normal and strike-slip earthquakes compared with reverse earthquakes, which is the opposite to that expected on the basis of mechanism alone. For large distances the imposed correction for style-of-faulting from Bommer et al. (2003) dominates and at great distances the predicted ground motions show the expected dependence on mechanism, i.e. reverse ground motions highest, followed by strike-slip motions and then normal motions. This distance-dependent effect of mechanism cannot be

captured by a simple scaling relation between the three mechanisms and consequently separate equations are presented for the three different mechanisms.

3.6 Uncertainties

For each of the derived models for the target region there are several sources contributing to the uncertainties in the ground motion estimates. For the median values of ground motion these are the following.

1. The spread of the original empirical models. Here the spread depends largely on the selection process if this spread is representative of those aspects of ground motion that need to be incorporated for the region under study. In addition, for some relations there is a trade-off between functional form and parameters and aleatory uncertainty, however, it is not considered here since its evaluation would require re-evaluation of the original empirical models.
2. The spread from using different parameter settings for conversions to adjust ground-motion models to a common set of predictor variables. Here, it is period dependent but magnitude and distance independent.
3. The uncertainty in the host-to-target factors. This has the following three components.
    a. The bias of the best-fitting stochastic model with respect to the empirical model. Loosely speaking, even the best-fitting stochastic model does not perfectly match the ground motions estimated by the host equations (Scherbaum et al., 2005b), which introduces additional variability contributing to the epistemic variability. The mismatch between the stochastic and empirical estimates is period, magnitude and distance dependent, however, Scherbaum et al. (2005b) provide a single (period, magnitude and distance) misfit value for each of their best-fit models and therefore here this variability is assumed to be period, magnitude and distance independent.
    b. The uncertainties generated from the spread of all those stochastic models that are considered valid models. Here we use the 100 best-fit stochastic models to characterise the host equation from Scherbaum et al. (2005b).
    c. The uncertainties coming from the numerous stochastic models for the target region (18 for Norway and 45 for Spain). This uncertainty is period, magnitude and distance dependent.

4. The uncertainty due to the fact that the adopted functional form does not perfectly match the computed target ground motion estimates at every point (e.g. Figure 6). This mismatch varies for period, magnitude and distance but here it is assumed to be magnitude and distance independent and equal to the standard deviation given by the regression analysis to derive the target ground motion models.

For the composite model of the aleatory variability the host-to-target conversion does not contribute. The source of uncertainties here are the following.

1. The spread of the standard deviations of the original host equations for the corrected magnitude and distance. It is period dependent and for some models (e.g. Abrahamson & Silva, 1997) magnitude dependent.
2. The additional variability due to the conversion of the independent parameters (magnitude, distance, style-of-faulting and component definition) in the host equations. It is period, magnitude and distance dependent.

Figure 15 and 16 compare the sizes of these different sources of uncertainties at twelve different magnitude and distance couples using stacked histograms for each model within the composite PGA model for southern Norway. Since the epistemic variance related from using different parameter settings for conversions to adjust ground-motion models to a common set of predictor variables (uncertainty number 2) and that related to the imperfect fit between the adopted functional form and the computed target ground motion estimates (uncertainty number 4) are much smaller than the other variances they are not included in Figure 15. In these figures variance (and not standard deviation) in terms of natural logarithms is plotted because variances are additive (standard deviations are not due to the square root) and therefore stacked histogram plots can be used.

Figure 15 shows that the epistemic uncertainty within the model is dominated by a lack of knowledge of the characterisation of the target region, which required the adoption of a wide range of stochastic models. In particular, the choice of three $\Delta\sigma$ values (5, 10 and 20 MPa [50, 100 and 200 bar]) leads to a large spread in stochastic estimates for the target region. This source of uncertainty is particularly big for large magnitude earthquakes at short distances (e.g. Mw 7.5 and d_{jb}=2km) but contributes most to the epistemic uncertainty for all magnitudes and distances. The next most important

contribution is due to the variability in the stochastic models for the host regions and can be large particularly at short distances. The other sources of epistemic variability do not contribute significantly to the overall uncertainty except the misfit (3a) between the stochastic and empirical estimates for the model of Sabetta & Pugliese (1996).

Figure 16 shows that the aleatory uncertainty is mainly due to the aleatoric variance within the original host empirical equations except for large magnitudes and/or short distances where the additional scatter introduced by the independent parameter conversions (almost entirely that due to the conversion for the distance metric) becomes particularly important.

Figures similar to Figure 15 and 16 were also drawn for the models for Spain but are not included here due to a lack of space. The figures showed similar results to those for Norway although the overall epistemic uncertainties were slightly lower.

4 Discussion and Conclusions

This article is a practical implementation of the composite ground-motion modelling methodology developed by Scherbaum et al. (2005a). The technique is applied to two regions of moderate seismicity where earthquake hazard nevertheless is important, namely southern Spain and southern Norway. The method is essentially one in which one or more empirical relations are transported from a host region to a target region. In the presented solution this is done in a comprehensive way in that it involves, as its central component, a host-to-target conversion based on the stochastic (random-vibration) method, based on a prior unification in terms of conversions for magnitude scale, distance metric, style-of-faulting distribution and component combination. These conversions are potentially important even when an empirical relation is used inside its host region, and even more so when it is used outside.

The role of all of these conversions are discussed by Bommer et al. (2005) in a logic-tree framework, which is also the way in which they are handled here, through a Monte Carlo approach. In this way the uncertainties are added, or propagated, allowing for the influence from uncertainties in each of the conversions. The host-to-target transformation based on the stochastic method is handled in a similar way, based on host-to-target differences in terms of source spectrum (here assumed to be Brune ω-square for both host and target), stress drop (admittedly with significant uncertainties because of poorly constrained values), geometrical

spreading, anelastic attenuation Q(f), and site conditions in terms of shear-wave velocity profiles and near-surface attenuation (κ). The distance conversions are, moreover, dependent on distributions of focal depths, faulting mechanisms and dip angles for earthquakes within the target region. The parameterizations and the uncertainties relating to all of these assumptions are discussed in detail in this article.

The stochastic models for each of the host equations used in this study have been obtained by a new and objective genetic algorithm search (Scherbaum et al., 2005b). They are associated with some uncertainty due to the 'subjective' exploration of the model parameter space and the trade-offs between different parameters within the stochastic models (Scherbaum et al., 2005b).

The host-to-target transformation and the other conversions documented and tested in this article essentially relaxes, if done properly, the usual condition of 'tectonic similarity' that earlier had to be (more or less) adhered to when seismic hazard analyses were performed in regions with no empirical strong-motion relations. The performance criteria is now simply reduced to how closely one can match the empirical host relations with stochastic predictions, which is not related to how different the tectonic conditions are for host and target regions. However, if the differences are large the conversion factors may become significant, although this does not in itself increase the uncertainty in the host-to-target conversions as compared to using regions with smaller geological differences.

The composite method developed by Scherbaum et al. (2005a) and implemented here therefore has interesting potentials for application to new regions. Admittedly, however, the method depends on a detailed parameterization where the assessment of both best estimates and related uncertainties may be difficult for regions that are poorly covered with seismological networks and studies. The ideal target regions are therefore those with a significant seismicity but still too low for providing reliable empirical strong-motion relations. Essentially this includes most seismically active regions outside of California and Japan.

Acknowledgements

This paper is contribution EG2/DT-10 from a series of studies inspired by participation in the PEGASOS project (Abrahamson et al., 2002). We thank Philip Birkhäuser, Jim Farrington, Andreas Hölker, Philippe Roth, Patrick Smit and Christian Sprecher for

providing a stimulating environment and continuous support for the development of ideas presented herein.

We thank Julián Garcia-Mayordomo, Belén Benito and Sergio Molina Palacios for some references containing parameters for southern Spain, Prof. M. Navarro for sending us a file with the profile for region 4 from Navarro et al. (1997), Dr K. W. Campbell for his encouragement with this work, for helping us reproduce his results and his comments on the revised version, Erik Hicks for providing the catalogue of Hicks et al. (2000) in electronic format, Dr D. M. Boore for giving us permission to disseminate modified versions of some of his SMSIM subroutines and for help in debugging CHEEP, all the staff and visitors at NORSAR for their help especially with computer programming difficulties and Julian Bommer for his careful review of a previous version of this article. CHEEP uses some subroutines from RANDLIB (Brown et al., 1997). In addition, we thank two anonymous reviewers of this revised version and the anonymous reviewer of a previous version for their valuable comments, which lead to improvements to the article.

John Douglas's contribution to this work was mainly conducted when he was visiting NORSAR under the European Community - Access to Research Infrastructure action of the Improving Human Potential Programme; he thanks the European Commission for their support. He also thanks Prof. N. N. Ambraseys for suggesting that he spent some time in Norway.

References

Abercrombie, R.E. (1995): Earthquake source scaling relationships from -1 to 5 ML using seismograms recorded at 2.5-km depth. Journal of Geophysical Research, 100, 24015-24036.

Abrahamson, N.A. & K.M. Shedlock (1997). Overview. Seismological Research Letters 68(1), 9-23.

Abrahamson, N.A., Birkhäuser, P., Koller, M., Mayer-Rosa, D., Smit, P., Sprecher, C., Tinic, S. and Graf, R. (2002), PEGASOS – a comprehensive probabilistic seismic hazard assessment for nuclear power plants in Switzerland. Proceedings of the Twelfth European Conference on Earthquake Engineering, London, Paper no. 633.

Abrahamson, N. A. and Silva, W. J., (1997), Empirical response spectral attenuation relations for shallow crustal earthquakes, Seismological Research Letters, 68(1), 94-127.

Akinci, A., Del Pezzo, E. and Ibáñez, J. M. (1995), Separation of scattering and intrinsic attenuation in southern Spain and western Anatolia (Turkey), Geophysical Journal International, 121(2), 337-353.

Ambraseys, N. N. and Free, M. W. (1997), Surface-wave magnitude calibration for European region earthquakes, Journal of Earthquake Engineering, 1(1), 1-22.

Ambraseys, N. N., Simpson, K. A. and Bommer, J. J. (1996), Prediction of horizontal response spectra in Europe, Earthquake Engineering & Structural Dynamics, 25, 371-400.

Atkinson, G. M. and Boore, D. M., (1997), Some comparisons between recent ground motion relations, Seismological Research Letters, 68(1), 24-40.

Atkinson, G. M. and Boore, D. M. (1998), Evaluation of models for earthquake source spectra in eastern North America, Bulletin of the Seismological Society of America, 88, 917-934.

Berge-Thierry, C., Cotton, F., Scotti, O., Griot-Pommera, D.-A. and Fukushima, Y., (2003), New empirical spectral attenuation laws for moderate European earthquakes, Journal of Earthquake Engineering, 7(2), 193-222.

Bommer, J. J., Douglas, J. and Strasser, F. O. (2003), Style-of-faulting in ground motion predictions, Bulletin of Earthquake Engineering, 1(2), 171-203.

Bommer, J. J., Scherbaum, F., Bungum, H., Cotton, F., Sabetta, F., and Abrahamson, N. A. (2005), On the use of logic trees for ground-motion prediction equations in seismic hazard analysis, Bulletin of the Seismological Society of America, 95(2), 377-389.

Boore, D. M. (1983), Stochastic simulation of high-frequency ground motion based on seismological models of the radiated spectra, Bulletin of the Seismological Society of America, 73, 1865-1893.

Boore, D. M. (2003), SMSIM – Fortran programs for simulating ground motions from earthquakes: Version 2.0 – A revision of OFR 96-80-A, A modified version of OFR 00-509, describing the program as of February 09, 2003 (version 2.20), U.S. Geological Survey.

Boore, D. M. and Joyner, W. B. (1997), Site amplifications for generic rock sites, Bulletin of the Seismological Society of America, 87(2), 327-341.

Boore, D. M., Joyner, W. B. and Fumal, T. E., (1997), Equations for estimating horizontal response spectra and peak acceleration from western North American earthquakes: A summary of recent work, Seismological Research Letters, 68(1), 128-153.

Brown, B. W., Lovato, J., Russell, K. and Venier, J. (1997), RANDLIB – Library of Fortran Routines for Random Number Generation, version 1.3, Department of Biomathematics, The University of Texas, M. D. Anderson Cancer Center.

Budnitz, R.J., G. Apostolakis, D.M. Boore, L.S. Cluff, K.J. Coppersmith, C.A. Cornell & P.A. Morris (1997). Recommendations for probabilistic seismic hazard analysis: guidance on uncertainty and use of experts. US Nuclear Regulatory Commission Report NUREG/CR-6372.

Bungum, H. and Alsaker, A. (1991), Source spectral scaling inversion for two earthquake sequences offshore western Norway, Bulletin of the Seismological Society of America, 81(2), 358-378.

Bungum, H., Alsaker, A., Kvamme, L. B. and Hansen, R. A. (1991), Seismicity and seismotectonics of Norway and nearby continental shelf areas, Journal of Geophysical Research, 96, 2249-2265.

Bungum, H., Dahle, A., Toro, G., McGuire, R. and Gudmestad, O. T. (1992), Ground motions from intraplate earthquakes, Proceedings of the10th World Conference on Earthquake Engineering, 2, 611-616.

Bungum, H., Lindholm, C.D., Dahle, A., Woo, G., Nadim, F., Holme, J.K., Gudmestad, O.T., Hagberg, T. & Karthigeyan, K. (2000). New seismic zoning maps for Norway, the North Sea and the U.K. Seismological Research Letters, 71, 687-697.

Bungum, H., Vaage, S. and Husebye, E. S. (1982), The Meløy earthquake sequence, northern Norway; source parameters and their scaling relations, Bulletin of the Seismological Society of America, 72(1), 197-206.

Byrkjeland, U., Bungum, H. and Eldholm, O. (2000). Seismotectonics of the Norwegian continental margin, Journal of Geophysical Research, 105, 6221-6236.

Cabañas, L., Lopez, M., Benito, B. and Jiménez, M. E. (2000), Estimation of PGA attenuation laws for Spain and Mediterranean region. Comparison with other ground motion models, Proceedings of the XXVII General Assembly of the European Seismological Commission. Lisbon, Portugal.

Campbell, K. W., (1997), Empirical near-source attenuation relationships for horizontal and vertical components of peak ground acceleration, peak ground velocity, and pseudo-absolute acceleration response spectra, Seismological Research Letters, 68(1), 154-179.

Campbell, K. W. (2003), Prediction of strong ground motion using the hybrid empirical method and its use in the development of ground-motion (attenuation) relations in eastern North America, Bulletin of the Seismological Society of America, 93(3), 1012-1033.

Campbell, K. W. (2004), Erratum to "Prediction of Strong Ground Motion Using the Hybrid Empirical Method and Its Use in the Development of Ground-Motion (Attenuation) Relations in Eastern North America", Bulletin of the Seismological Society of America, 94(6), 2418.

Campbell, K. W. and Bozorgnia, Y. (2003a), Updated near-source ground-motion (attenuation) relations for the horizontal and vertical components of peak ground acceleration and acceleration response spectra, Bulletin of the Seismological Society of America, 93(1), 314-331.

Campbell, K. W. and Bozorgnia, Y. (2003b), Erratum: Updated near-source ground-motion (attenuation) relations for the horizontal and vertical components of peak ground acceleration and acceleration response spectra, Bulletin of the Seismological Society of America, 93(3), 1413.

Canas, J. A. and Pujades, L., Badal, J., Payo, G., de Miguel, F., Vidal, F., Alguacil, G., Ibañez, J. and Morales, J. (1991), Lateral variation and frequency dependence of coda-Q in the southern part of Iberia, Geophysical Journal International, 107, 57-66.

Chael, E. P. and Kromer, R. P. (1988), High-frequency spectral scaling of main shock/aftershock sequence near the Norwegian coast, Bulletin of the Seismological Society of America, 78(2), 561-570.

Chopra, A. K. (1995), Dynamics of structures: theory and applications to earthquake engineering, Prentice Hall, Englewood Cliffs, N. J.

Cotton, F., Scherbaum, F., Bommer, J. J. and Bungum, H. (2005), Criteria for selecting and adjusting ground-motion models for specific target regions: Application to central Europe and rock sites, Journal of Seismology, submitted.

Dahle, A., Bungum, H. and Kvamme, L. B. (1990), Attenuation models inferred from intraplate earthquake recordings, Earthquake Engineering & Structural Dynamics, 19, 1125-1141.

Dahle, A., Bungum, H. and Kvamme, L. B. (1991), Empirically derived PSV spectral attenuation models for intraplate conditions, European Earthquake Engineering, 3, 42-52.

De Miguel, F., Ibáñez, J. M., Alguacil, G., Canas, J. A., Vidal, F., Morales, J., Peña, J. A., Posadas, A. M. and Luzón, F. (1992), 1-18Hz Lg attenuation in the Granada basin (southern Spain), Geophysical Journal International, 111(2), 270-280.

Douglas, J. (2001), A critical reappraisal of some problems in engineering seismology, Ph.D. thesis, University of London, London, United Kingdom.

Douglas, J. (2003a), Earthquake ground motion estimation using strong-motion records: A review of equations for the estimation of peak ground acceleration and response spectral ordinates, Earth-Science Reviews, 61, 43-104.

Douglas, J. (2003b), A note on the use of strong-motion data from small magnitude earthquakes for empirical ground motion estimation, Proceedings of Skopje Earthquake – 40 Years of European Earthquake Engineering (SE40EEE).

Frohlich, C. and Apperson, K. D. (1992), Earthquake focal mechanisms, moment tensors, and the consistency of seismic activity near plate boundaries, Tectonics, 11, 279-296.

Galindo-Zaldívar, J., Jabaloy, A., González-Lodeiro, F. and Aldaya, F. (1997), Crustal structure of the central sector of the Betic Cordillera (SE Spain), Tectonics, 16(1), 18-37.

García-García, J. M., Vidal, F., Romacho, M. D., Martín-Marfil, J. M., Posadas, A. and Luzón, F. (1996), Seismic source parameters for microearthquakes of the Granada basin (southern Spain), Tectonophysics, 261(1-3), 51-66.

García-García, J. M., Romacho, M. D., Jiménez, A. and Posadas, A. M. (2002), Determination of near-surface attenuation, with the κ parameter, in the Granada basin, 3 Asamblea Hispano-Portuguesa de Geodesia y Geofisica, Valencia, S05, pp. 489-493.

Garcia-Fernandez, M. and Canas, J. A. (1991), Estimation of regional values of peak ground acceleration from short-period seismograms, Proceedings of the Fourth International Conference on Seismic Zonation, vol. II, 533-539.

Garcia-Fernandez, M. and Canas, J. A. (1995), Regional peak ground acceleration estimates in the Iberian peninsula, Proceedings of the Fifth International Conference on Seismic Zonation, vol. II, 1029-1034.

Grant, F. S. & West, G. F. (1965), Interpretation Theory in Applied Geophysics, McGraw-Hill Book Company, New York.

Hansen, R. A., Bungum, H. and Alsaker, A. (1989), Three recent larger earthquakes offshore of Norway, Terra Nova, 1, 284-295.

Hicks, E. C., Bungum, H. and Lindholm, C. D. (2000), Stress inversion of earthquake focal mechanism solutions from onshore and offshore Norway, Norsk Geologisk Tidsskrift, 80, 235-250.

Hiramatsu, Y., Yamanaka, H., Tadokoro, K., Nishigami, K. and Ohmi, S. (2002), Scaling law between corner frequency and seismic moment of microearthquakes: Is the breakdown of the cube law a nature of earthquakes? Geophysical Research Letters, 29(8), 10.1029/2001GL013894.

Ibáñez, J. M., Del Pezzo, E., De Miguel, F., Herraiz, M., Alguacil, G. and Morales, J. (1990), Depth-dependent seismic attenuation in the Granada zone (southern Spain), Bulletin of the Seismological Society of America, 80(5), 1232-1244.

Ibáñez, J. M., Del Pezzo, E., Alguacil, G., De Miguel, F., Morales, J., De Martina, S., Sabbarese, C. and Posadas, A. M.. (1993), Geometrical spreading function for short-period S and coda waves recorded in southern Spain, Physics of the Earth and Planetary Interiors, 80(1-2), 25-36.

Ide, S. and Beroza, G. C. (2001), Does apparent stress vary with earthquake size?, Geophysical Research Letters, 28(17), 3349-3352.

Kvamme, L. B. and Havskov, J. (1989), Q in southern Norway, Bulletin of the Seismological Society of America, 79(5), 1575-1588.

Kvamme, L. B., Hansen, R. A. and Bungum, H. (1995), Seismic-source and wave-propagation effects of Lg waves in Scandinavia, Geophysical Journal International, 120, 525-536.

Laske, G., Masters, G. and Reif, C. (2003), CRUST 2.0: A New Global Crustal Model at 2x2 Degree, on the Internet at: http://mahi.ucsd.edu/Gabi/rem.html.

Lokshtanov, D. E., Ruud, B. O. and Husebye, E. S. (1991), The upper crust low velocity layer; a Rayleigh (Rg) phase velocity study from SE Norway, Terra Nova, 3(1), 49-56.

Lussou, P., Bard, P.-Y., Cotton, F. and Fukushima, Y., (2001), Seismic design regulation codes: Contribution of K-Net data to site effect evaluation, Journal of Earthquake Engineering, 5(1), 13-34.

Martín Martín, A. J. (1989), Probabilistic seismic hazard analysis and damage assessment in Andalusia (Spain), Tectonophysics, 167, 235-244.

Mayeda, K. and Walter, W. R. (1996), Moment energy, stress drop, and source spectra of western United States earthquakes from regional coda envelopes, Journal of Geophysical Research, 101(B5), 11195-11208.

Mezcua, J., Herraiz, M. and Buforn, E. (1984), Study of the 6 June 1977 Lorca (Spain) earthquake and its aftershock sequence, Bulletin of the Seismological Society of America, 74(1), 167-179.

Morales, J., Singh, S. K. and Ordaz, M. (1996), Analysis of the Granada (Spain) earthquake of 24 June 1984 (M=5) with emphasis on seismic hazard in the Granada basin, Tectonophysics, 257(2-4), 253-263.

Morales, J., Benito, B. and Luján, M. (2003), Expected ground motion in the south-east of Spain due to an earthquake in the epicentral area of the 1910 Adra earthquake, Journal of Seismology, 7(2), 175-192.

Navarro, M., Corchete, V., Badal, J., Canas, J. A., Pujades, L. and Vidal, F. (1997), Inversion of Rg waveforms recorded in southern Spain, Bulletin of the Seismological Society of America, 87(4), 847-865.

Ottemöller, L. and Havskov, J. (2003), Moment Magnitude Determination for Local and Regional Earthquakes Based on Source Spectra, Bulletin of the Seismological Society of America, 93(1), 203-214.

Oye, V., H. Bungum and M. Roth (2005): Source parameters and scaling relations for mining related seismicity within the Pyhäsalmi ore mine, Finland. Bulletin of the Seismological Society of America, in press.

Pačėsa, A. (1999), Near-surface attenuation in Norway and noise studies in Lithuania and Israel and status of seismology in Lithuania, M.Sc. thesis, Institute of Solid Earth Physics, University of Bergen, Norway.

Payo, G., Badal, J., Canas, J. A., Corchete, V., Pujades, L. and Serón, F. J. (1990), Seismic attenuation in Iberia using the coda-Q method, Geophysical Journal International, 103(1), 135-145.

Pujades, L. G., Canas, J. A., Egozcue, J. J., Puigvi, M. A., Gallart, J., Lana, X., Pous, J. and Casas, A. (1990), Coda-Q distribution in the Iberian peninsula, Geophysical Journal International, 100(2), 285-301.

Pujades, L. G., Ugalde, A., Canas, J. A., Navarro, M., Badal, F. J. and Corchete, V. (1997), Intrinsic and scattering attenuation from observed seismic coda in the Almeria basin (southeastern Iberian peninsula), Geophysical Journal International, 129(2), 281-291.

Sabetta, F. and Pugliese, A. (1996), Estimation of response spectra and simulation of nonstationary earthquake ground motions, Bulletin of the Seismological Society of America, 86(2), 337-352.

Sadigh, K., Chang, C.-Y., Egan, J. A., Makdisi, F. and Youngs, R. R., (1997), Attenuation relationships for shallow crustal earthquakes based on California strong motion data, Seismological Research Letters, 68(1), 180-189.

Scherbaum, F., Cotton, F. and Smit, P. M. (2004a), On the use of response spectral-reference data for the selection of ground-motion models for seismic-hazard analysis in

regions of moderate seismicity: The case of rock motion, Bulletin of the Seismological Society of America, 94(6), 2164-2185.

Scherbaum, F., Schmedes, J. and Cotton, F. (2004b), On the conversion of source-to-site distance measures for extended earthquake source models, Bulletin of the Seismological Society of America, 94(3), 1053-1069.

Scherbaum, F. J.J. Bommer, H. Bungum, F. Cotton and N.A. Abrahamson (2005a), Composite ground-motion models and logic-trees: Methodology, sensitivities and uncertainties. Bulletin of the Seismological Society of America, 95(5), 1575-1593, doi: 10.1785/0120040229

Scherbaum, F., Cotton, F. and Staedtke, H. (2005b), The estimation of minimum-misfit stochastic models from empirical ground-motion prediction equations, Bulletin of the Seismological Society of America, in press.

Sereno, T. J., Bratt, S. R. and Bache, T. C. (1988). Simultaneous inversion of regional wave spectra for attenuation and seismic moment in Scandinavia, Journal of Geophysical Research, 93, 2019–2035.

Silva, W., Martin, G., Abrahamson, N. and Kircher, C. (1998), Reassessment of site coefficients and near-fault factors for building code provisions: Program Element II, 98-HQ-GR-1010.

Singh, S. K., Ordaz, M., Lindholm, C. D. and Havskov, J. (1990), Seismic hazard in southern Norway, Seismo-Series No. 46, Institute of Solid Earth Physics, Seismological Observatory, University of Bergen, Norway.

Sjøgren, B., Øfsthus, A. and Sandberg, J. (1979), Seismic classification of rock mass qualities, Geophysical Prospecting, 27(2), 409-442.

Stepp, J. C., Wong, I., Whitney, J., Quittmeyer, R., Abrahamson, N., Toro, G., Youngs, R., Coppersmith, K., Savy, J., Sullivan, T. and Yucca Mountain PSHA Project members (2001), Probabilistic seismic hazard analyses for ground motions and fault displacement at Yucca Mountain, Nevada, Earthquake Spectra, 17(1), 113-151.

Stich, D., Ammon, C. J. and Morales, J. (2003), Moment tensor solutions for small and moderate earthquakes in the Ibero-Maghreb region, Journal of Geophysical Research, 108(B3), 2148, doi: 10.1029/2002JB002057.

Udias, A. and Munoz, D. (1979) The Andalusian earthquake of 25 December 1884, Tectonophysics, 53, 291-299.

Zappone, A., Fernàndez, M., García-Dueñas, V. and Burlini, L. (2000), Laboratory measurements of seismic P-wave velocities on rocks from the Betic chain (southern Iberian Peninsula), Tectonophysics, 317, 259-272.

Zobin, V. M. & Havskov, J. (1995), Source spectral properties of small earthquakes in the northern North Sea, Tectonophysics, 248(3-4), 207-218.

Tables

Table 1: Distribution of 45 shallow earthquakes in southern Spain with respect to mechanism using data from Stich et al. (2003) and classification scheme of Frohlich & Apperson (1992). Three events from the catalogue had intermediate depths and were not used.

Mechanism	Number of earthquakes
Normal	3 (6.7%)
Strike-slip	10 (22.2%)
Thrust	3 (6.7%)
Odd	29 (64.4%)

Table 2: Distribution of earthquakes in southern Norway with respect to mechanism using data from Hicks et al. (2000) and classification scheme of Frohlich & Apperson (1992).

Mechanism	Number of earthquakes
Normal	9 (13.4%)
Strike-slip	9 (13.4%)
Thrust	17 (25.3%)
Odd	32 (47.8%)

Table 3: Parameters of the stochastic models for southern Spain and southern Norway. Where multiple values are used, weights are given in parantheses.

Parameter	Southern Spain	Southern Norway
Source spectrum	Brune ω-square, point source	Brune ω-square, point source
Stress drop, $\Delta\sigma$ (bar)	50 (0.30), 100 (0.40), 200 (0.30)	50 (0.30), 100 (0.40), 200 (0.30)
Geometric attenuation	R^{-1}; R<40km $R^{-0.5}$; R≥40km	R^{-1}; R<70km R^{0}; 70≤R<130km $R^{-0.5}$; R≥130km
Source duration, T_s (s)	$1/f_0$	$1/f_0$
Path duration, T_p (s)	0.05R	0; R≤10km 0.16R; 10<R≤70km -0.03R; 70<R≤130km 0.04R; R>130km
Path attenuation, Q	$112.5f^{0.85}$ (0.2), $100f^{0.70}$ (0.2), $153f^{0.66}$ (0.2), $105f^{0.93}$ (0.2), $63f^{0.88}$ (0.2)	$560f^{0.26}$ (0.5), $438f^{0.71}$ (0.5)
Shear-wave velocity, β_s (km/s)	3.7	4.0
Density, ρ_s (kg/m^3)	2900	3100
Site attenuation, κ_0 (s)	0.006 (0.3), 0.02 (0.4), 0.05 (0.3)	0.008 (0.3), 0.017 (0.4), 0.026 (0.3)
Site amplification method	Quarter-wavelength	Quarter-wavelength
Local site profile ($V_{s,30}$)	Navarro et al. (1997) (1870m/s)	Eastern North America hard rock (2800m/s)

Table 4: Equations chosen for the derivation of composite equations for the two target regions, region where most data used was recorded (WNA is western North America) and the choices of independent parameters used.

Equation	Region	Abbreviation	Parameters
Abrahamson & Silva (1997)	WNA	AS97	F=0 and HW=0
Ambraseys et al. (1996)	Europe	AETAL96	S_A=0 and S_S=0
Berge-Thierry et al. (2003)	Europe+ WNA	BTETAL03	Used coefficients for site class 1
Boore et al. (1997)	WNA	BETAL97	$V_{s,30}$=620m/s, SS=1 and RV=0
Campbell & Bozorgnia (2003a,b)	WNA	CB03	S_{VFS}=0, S_{SR}=0.5, S_{FR}=0.5, F_{RV}=0, F_{TH}=0 (no hanging wall effect)
Lussou et al. (2001)	Japan	LETAL01	Used coefficients for site class 2
Sabetta & Pugliese (1996)	Italy	SP96	S_1=0 and S_2=0

Figure Captions

Figure 1: Comparison of estimated ground motions in eastern North America derived from western North American equations using CHEEP (black dots) presented here and the estimates given by the equations derived by Campbell (2003, 2004) for M_w=5.0, 6.0, 7.0 and 8.0 (solid lines) and d_r=30km.

Figure 2: Depth distribution of shallow earthquakes in the catalogue of Stich et al. (2003) for the region 36ºN-39ºN and 0º-6ºW.

Figure 3: Attenuation factor exp(-α), where $\alpha=\pi fR/\beta_c Q$ where f is frequency, R is hypocentral distance (taken as 100km) and β_c is shear-wave velocity (assumed to be 3.5km/s) from published estimates for southern Spain. The equations used are: $Q(f)=112.5f^{0.85}$ (Ibáñez et al., 1990), $Q(f)=100f^{0.7}$ (Pujades et al., 1990), $Q(f)=153f^{0.66}$ (Canas et al., 1991), $Q(f)=105f^{0.93}$ (De Miguel et al., 1992) and $Q(f)=63f^{0.88}$ (Pujades et al., 1997).

Figure 4: Attenuation factor exp(-α), where $\alpha=\pi fR/\beta_c Q$ where f is frequency, R is hypocentral distance (taken as 100km) and β_c is shear-wave velocity (assumed to be 3.5km/s) from published estimates for Norway.

Figure 5: Depth distribution of earthquakes in the catalogue of Hicks et al. (2000) for the region 58ºN-64ºN and 0º-12ºE for normal, strike-slip and thrust faulting.

Figure 6: Comparison of the estimated PGAs derived for southern Spain derived from the equation of Abrahamson & Silva (1997) (dots) compared with the predicted PGAs from the fitted equation (lines) for M_w=4.5, 5.5, 6.5 and 7.5.

Figure 7: Estimated response spectra for an M_w=6 earthquake at d_{jb}=20km in the host regions (solid grey lines) and in southern Spain (dotted black lines) using the equations of Abrahamson & Silva (1997) and Lussou et al. (2001). This figure shows the effect of the host-to-target conversion.

Figure 8: Graphs of the estimated ground motion for a M_w=6 earthquake using the derived ground motion models for Spain for each of the host equations for a) PGA and b) SA at 1s.

Figure 9: Estimated response spectra using the derived equations for Spain for an M_w=6 earthquake at d_{jb}=20km.

Figure 10: Comparison between the PGA predicted by two of the equations (Berge-Thierry et al., 2003; Campbell and Bozorgnia, 2003a, b) as adopted for southern Spain and those predicted using the equations of Garcia-Fernandez & Canas (1991,1995) and Cabañas et al. (2000) for M_w=5 and 7.

Figure 11: As for Figure 8 but for Norway (normal mechanism earthquakes).

Figure 12: As for Figure 9 except for Norway (normal mechanism earthquakes).

Figure 13: Comparison of the predicted PGAs and SA at 1s from two of the relations (Berge-Thierry et al., 2003; Campbell and Bozorgnia, 2003a, b) as adopted for

Norway (strike-slip faulting) and the predicted ground motions from the models presented by Bungum et al. (1992) (constant 5 MPa [50 bar] stress drop model and increasing stress drop model) and Dahle et al. (1991) (no equation for PGA presented) for M_w=5 and M_w=7. A focal depth of 10km was assumed for the relations of Bungum et al. (1992) and Dahle et al. (1991).

Figure 14: Comparison of the predicted PGAs and SA at 1s from the relations (Campbell and Bozorgnia, 2003a, b) as adopted for Norway for the three styles-of-faulting: normal, strike-slip and reverse.

Figure 15: Epistemic variances within the composite model for the median PGA for southern Norway. Each small stacked histogram graph is for a given magnitude (see y-axis of the overall graph) and distance (see x-axis of the overall graph) and each column is for a given ground motion model, which from left to right are: AS97, AETAL96, BTETAL03, BETAL97, CB03, LETAL01 and SP96. The contributions to the overall variance are identified by the shade of grey and are given in the same order as in the text (see legend in bottom right plot).

Figure 16: Aleatory variances with the composite PGA model for southern Norway. See caption of Figure 15 for explanation.

Figures

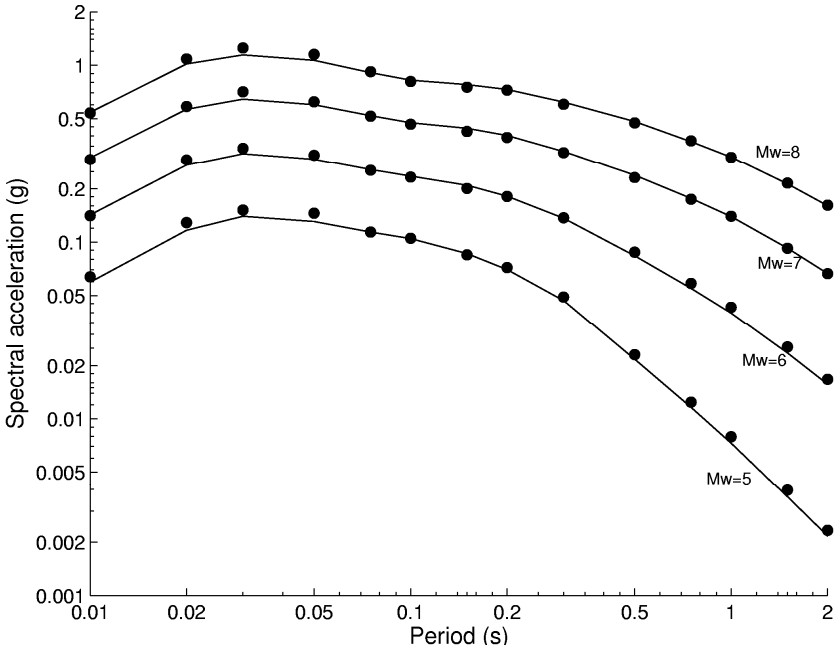

Figure 1

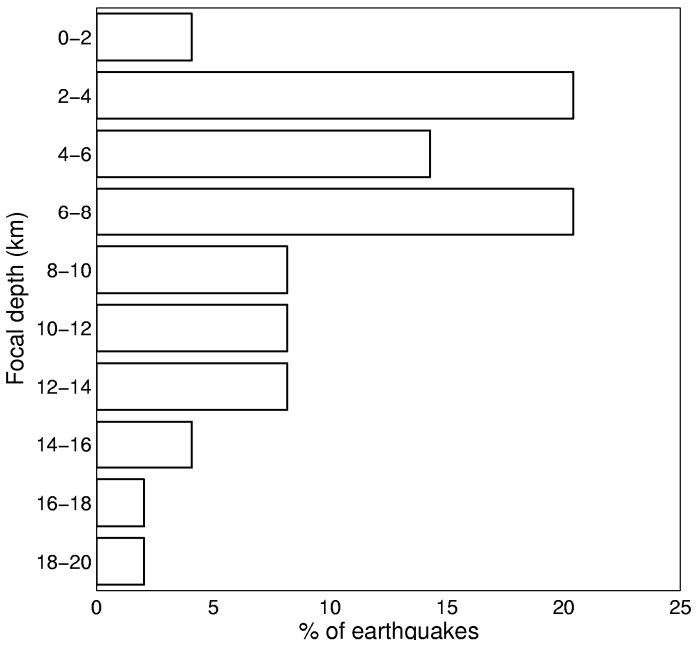

Figure 2

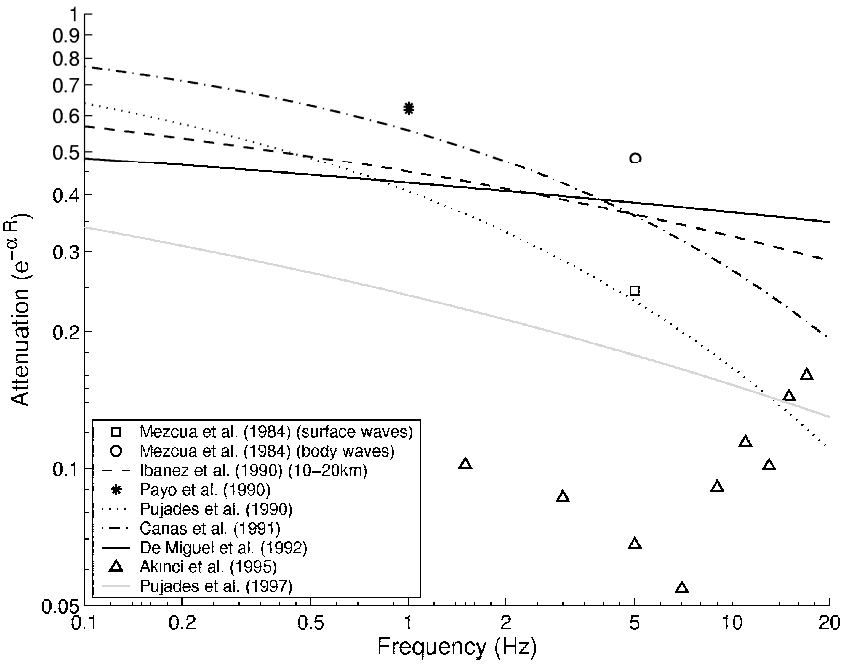

Figure 3

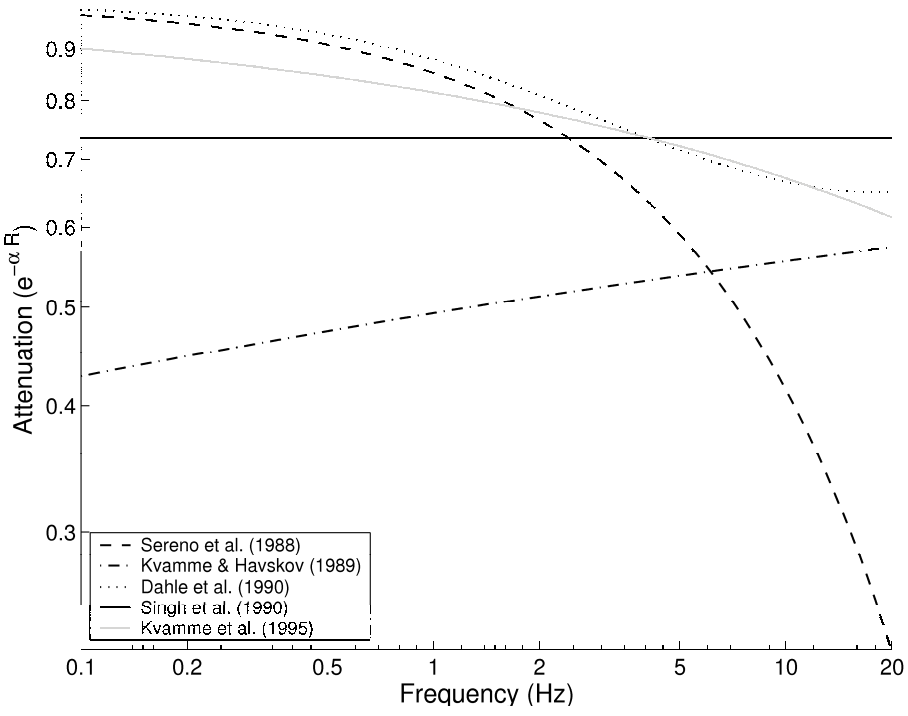

Figure 4

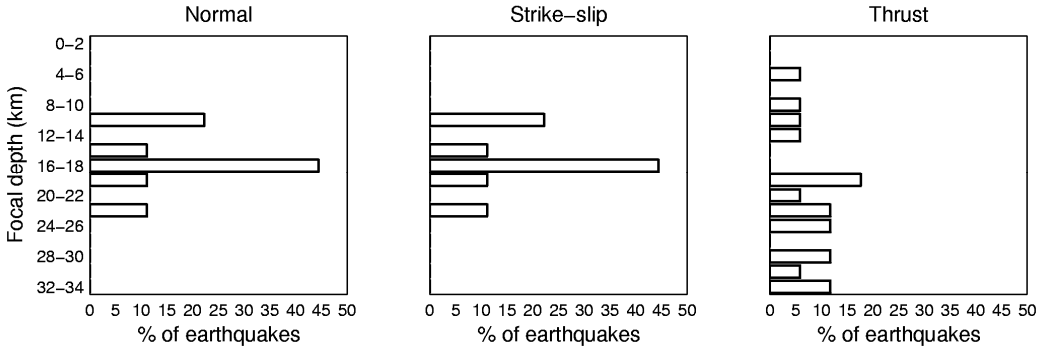

Figure 5

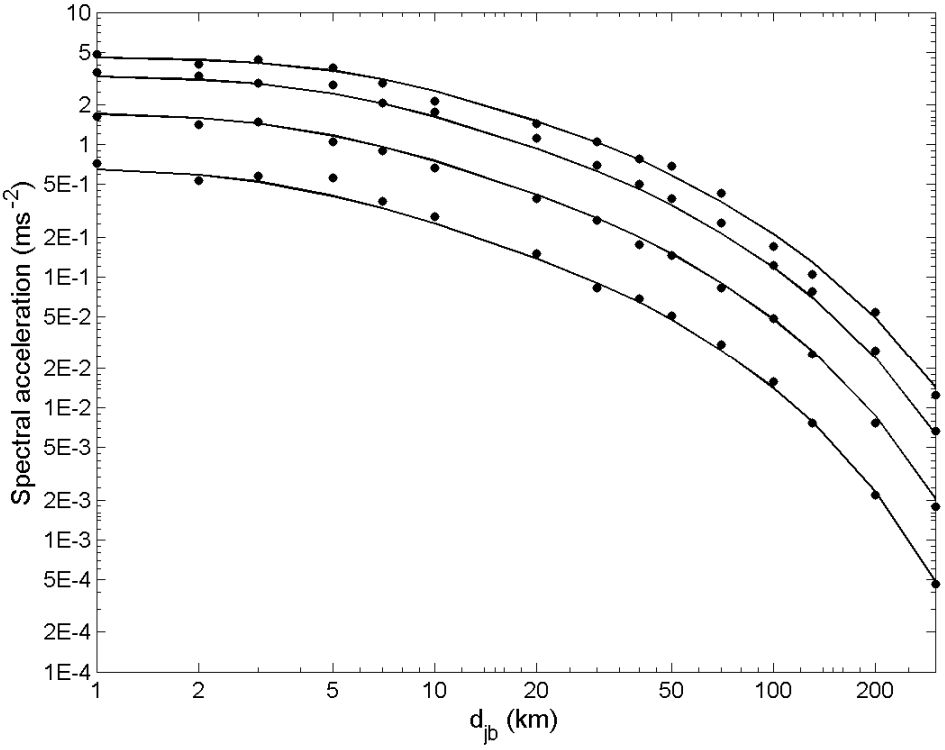

Figure 6

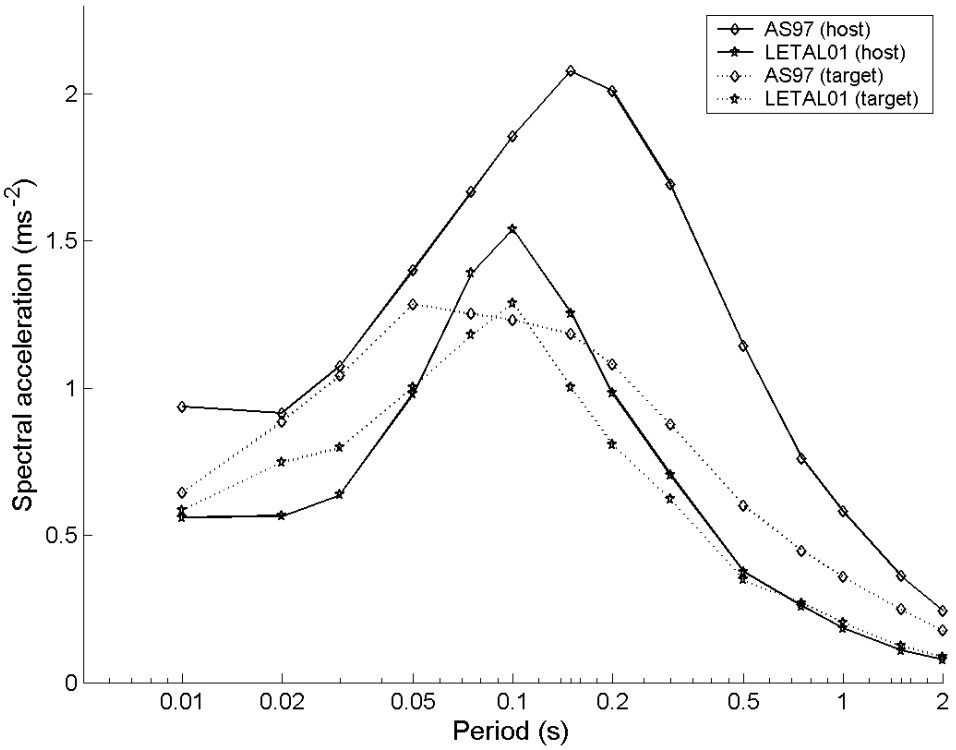

Figure 7

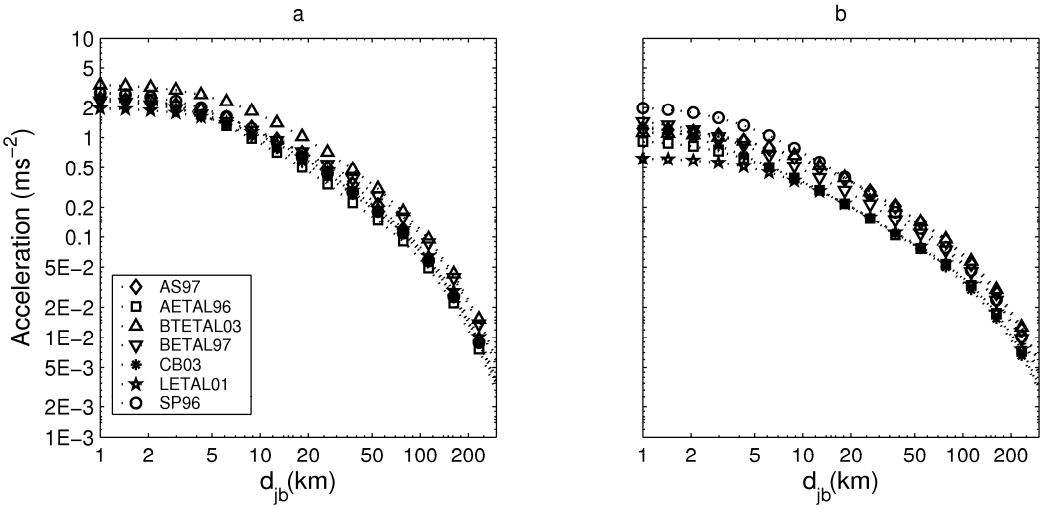

Figure 8

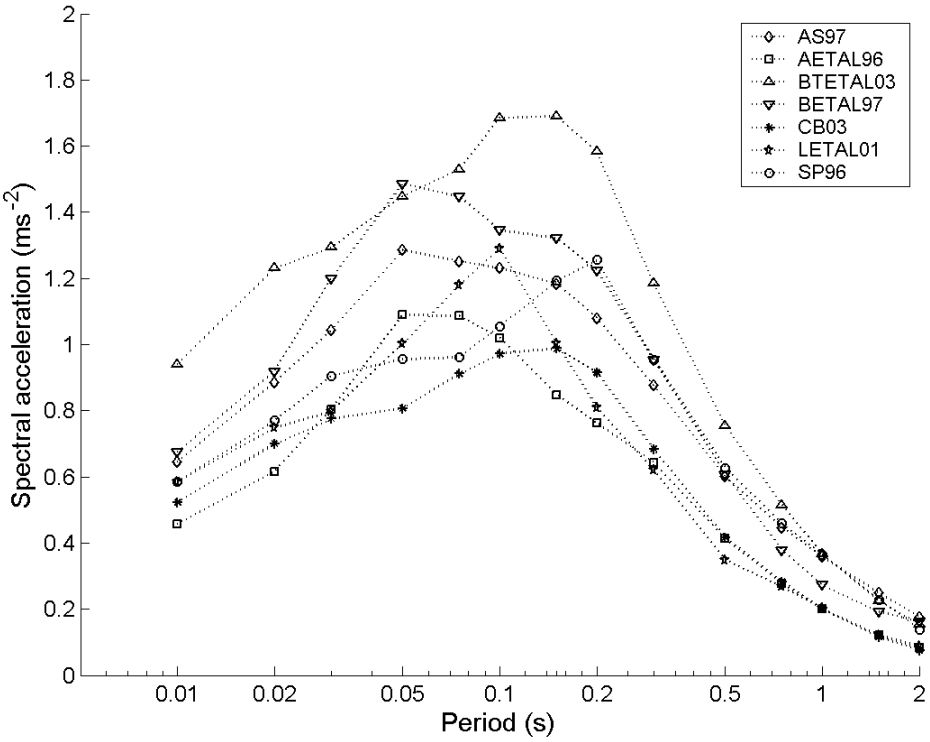

Figure 9

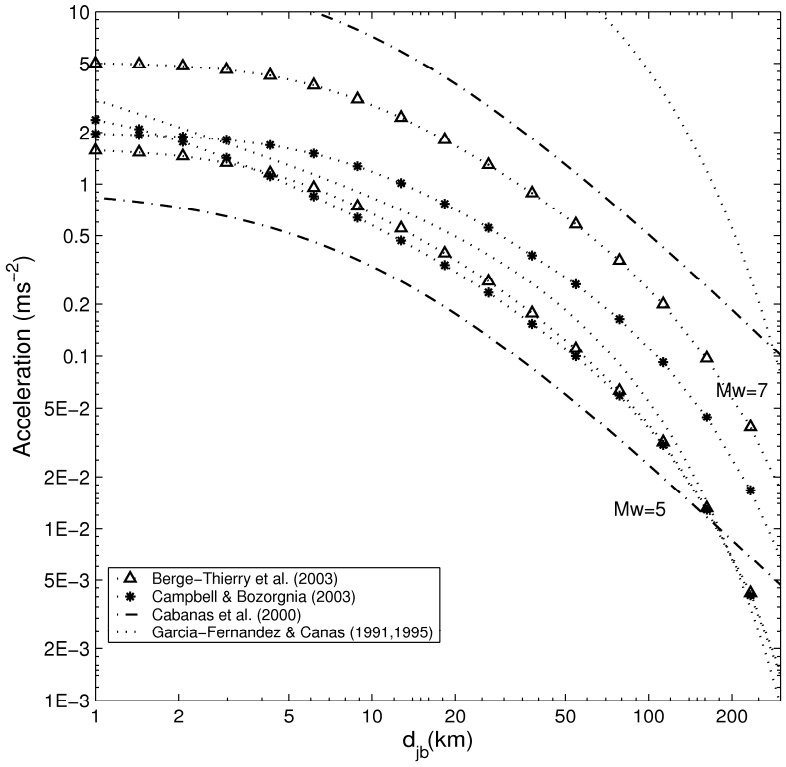

Figure 10

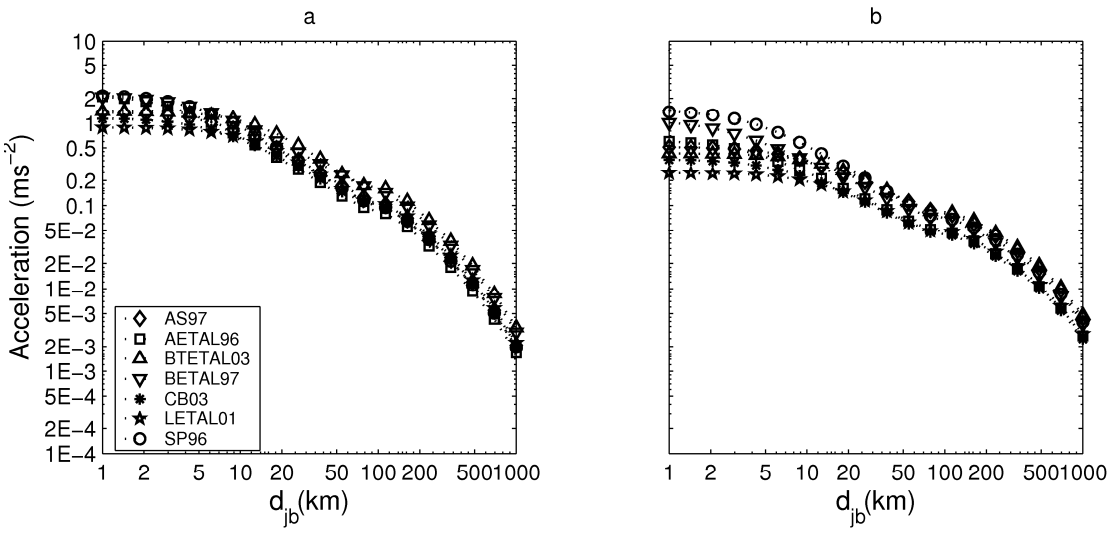

Figure 11

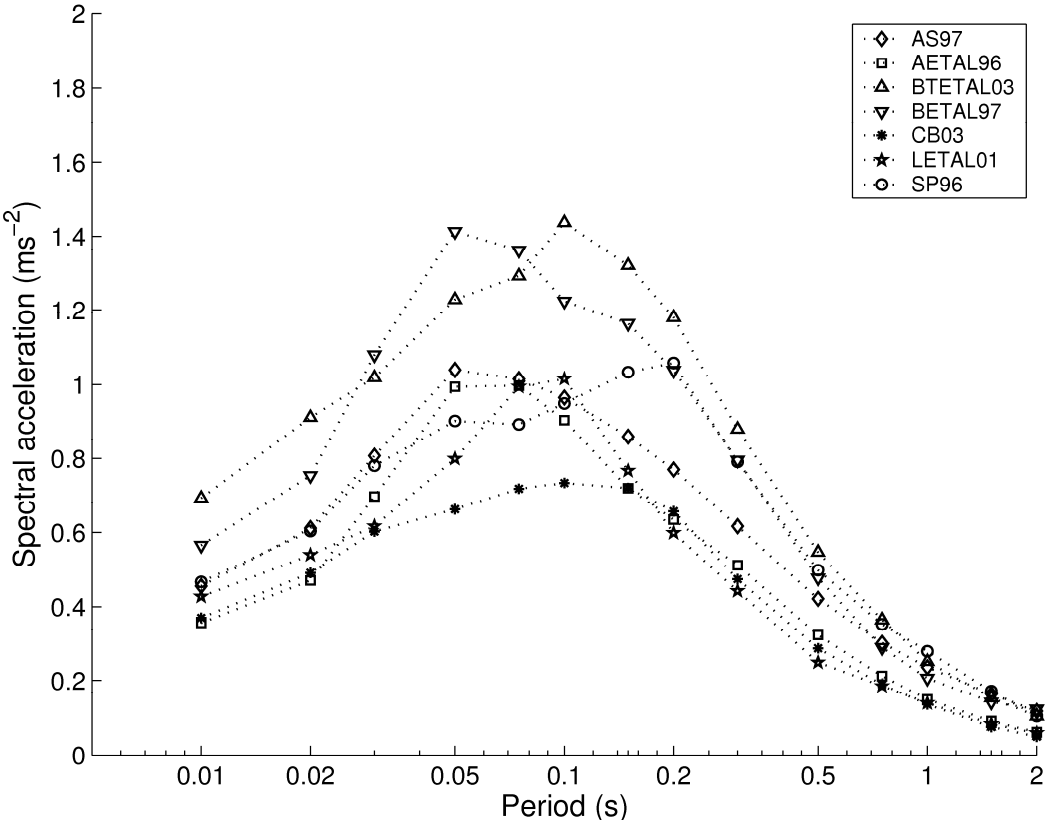

Figure 12

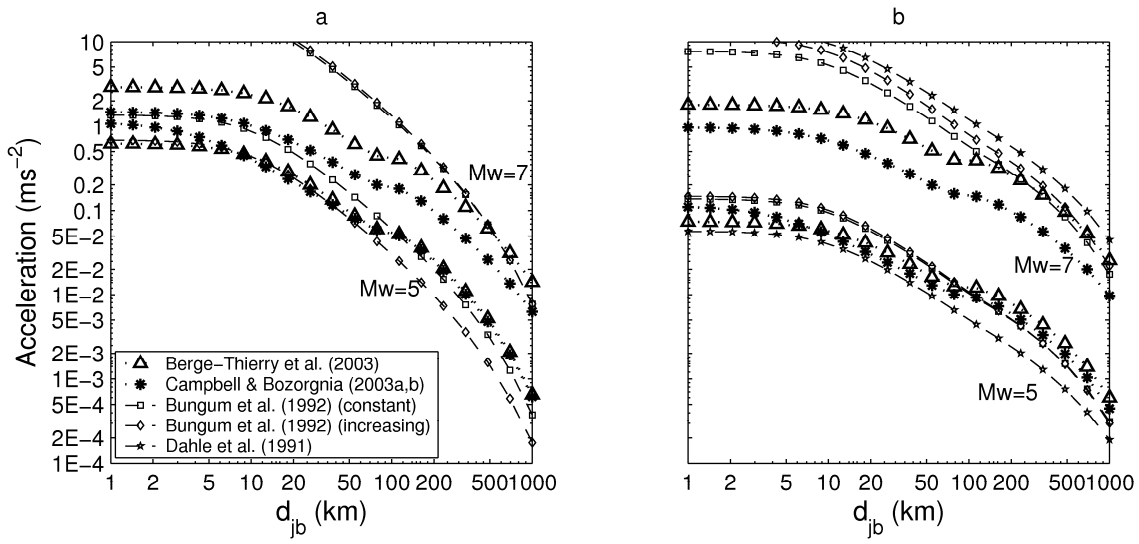

Figure 13

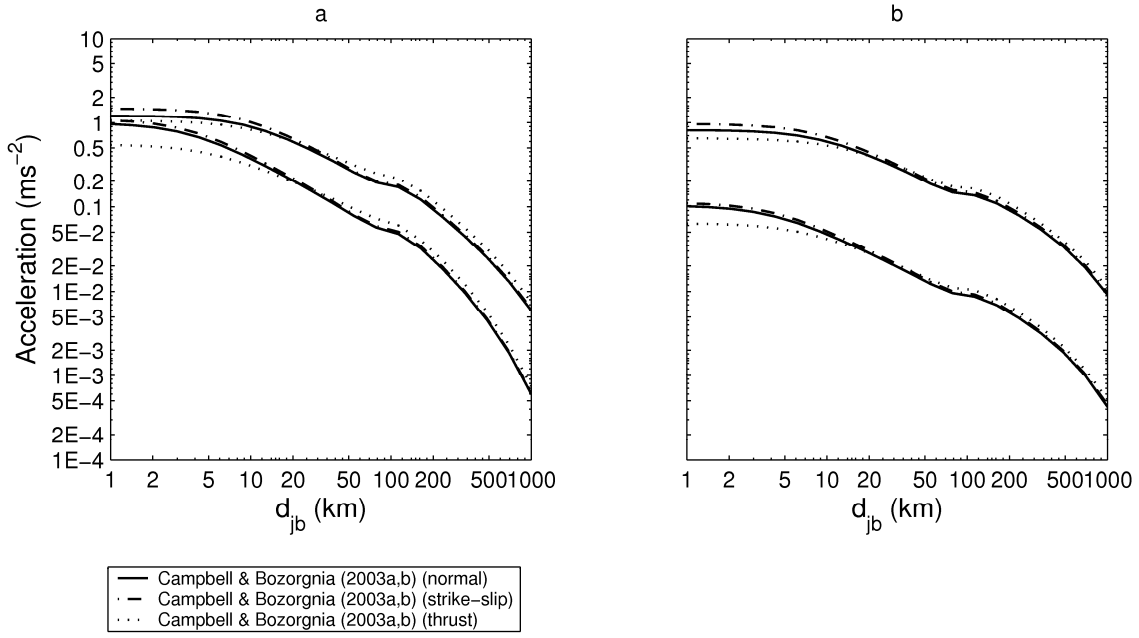

Figure 14

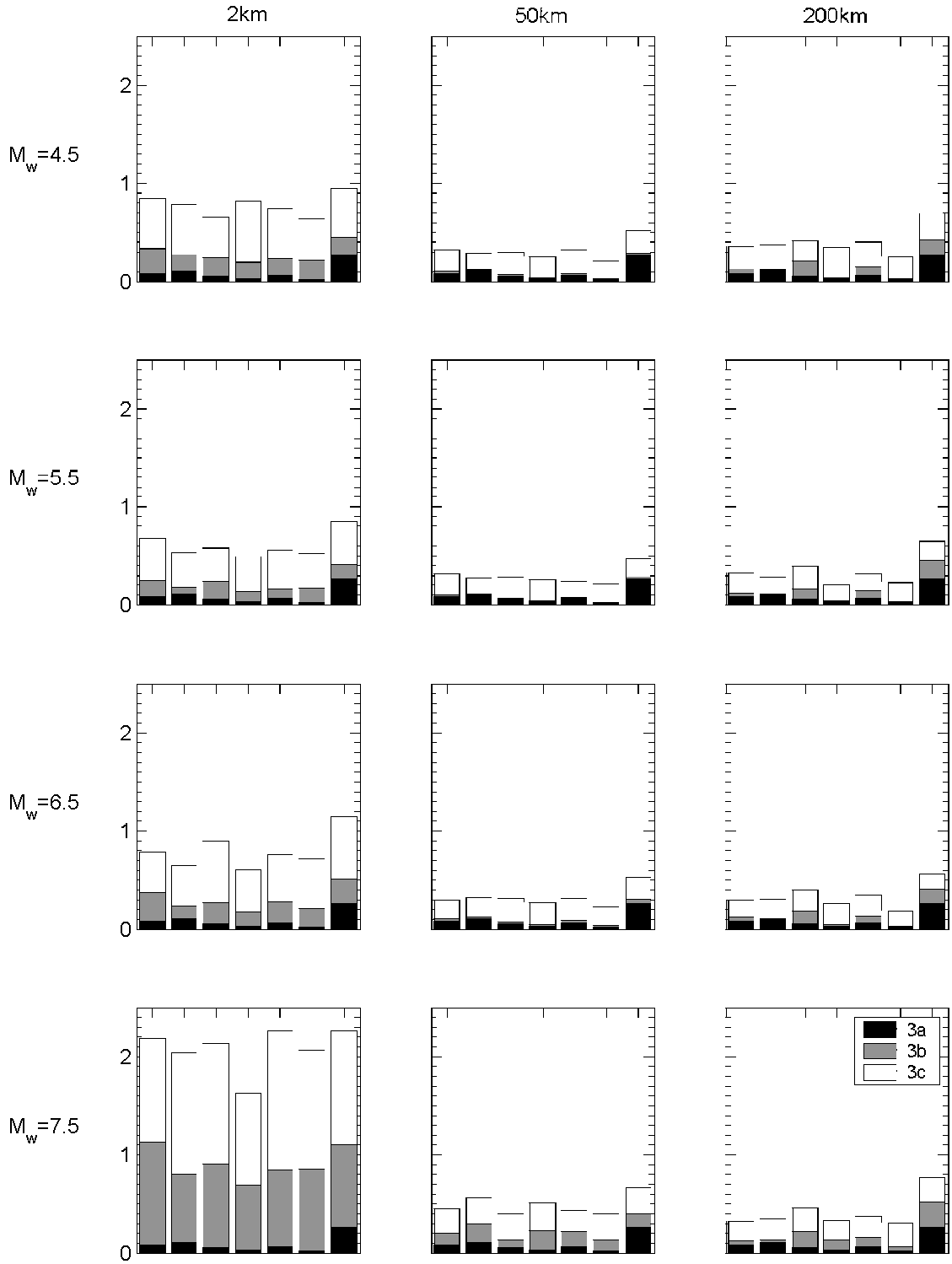

Figure 15

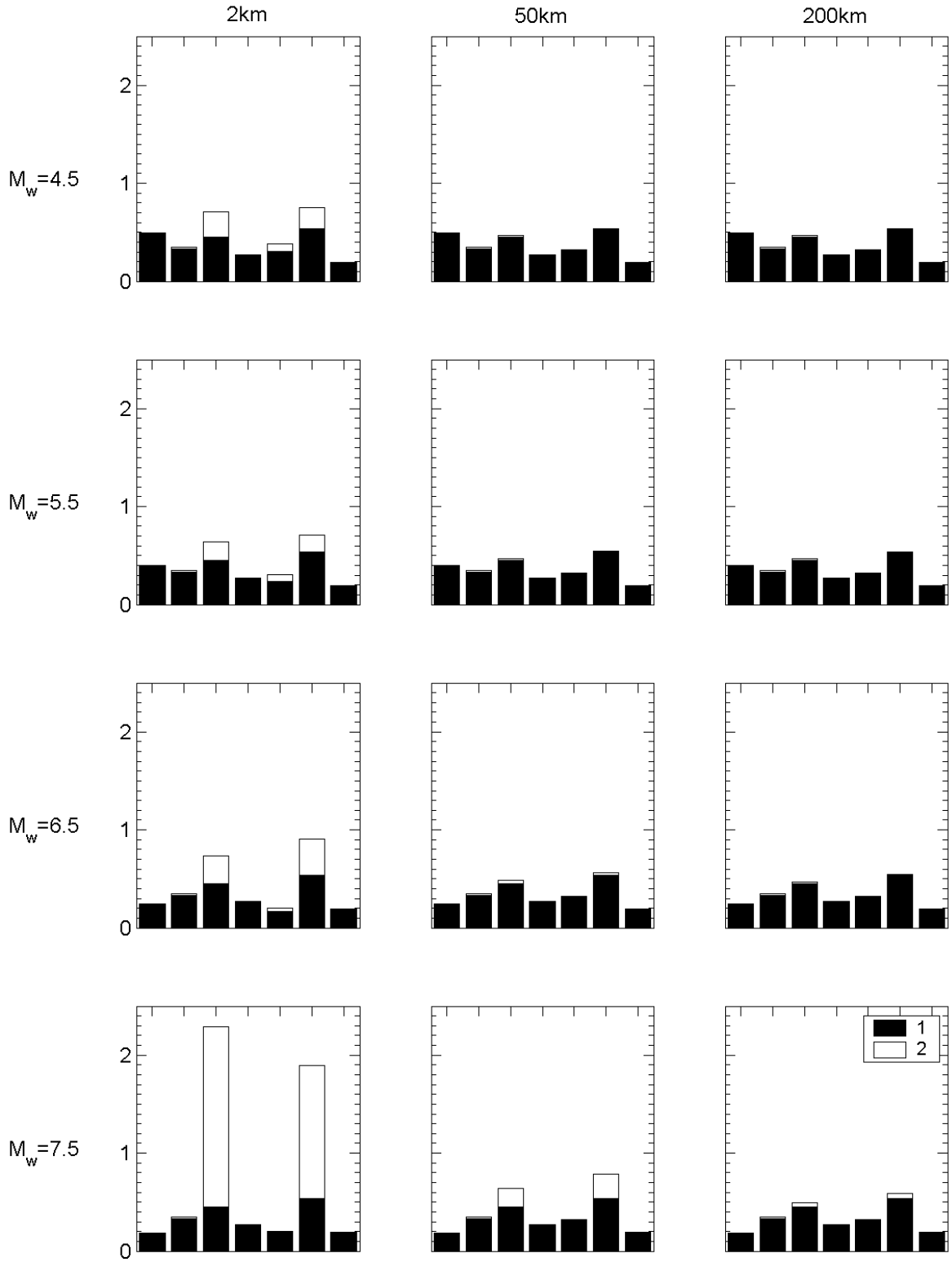

Figure 16